Determining the Relative Average Degree of Channelization (RADC) for Starch Granules of Five Maize Inbred Lines

A Thesis

Presented in Partial Fulfillment of the Requirements for the

Degree of Master of Science

with a

Major in Food Science

in the

College of Graduate Studies

University of Idaho

by

Yu-Hui Chao

Major Professor: Kerry C. Huber, Ph.D.

Committee Members: Girish Ganjyal, Ph.D.; Steven McGeehan, Ph.D.; James E. Nelson, M.S.

Department Administrator: Barbara Rasco, Ph.D.

August 2015

AUTHORIZATION TO SUBMIT THESIS

This Thesis of Yu-Hui Chao, submitted for the degree of Master of Science with a Major in Food Science and titled "Determining the Relative Average Degree of Channelization (RADC) for Starch Granules of Five Maize Inbred Lines," has been reviewed in final form. Permission, as indicated by this signatures and dates below, is now granted to submit final copies to the College of Graduates Studies for approval.

Major Professor: _____ Date: _____
Kerry C. Huber, Ph.D.

Committee Members: _____ Date: _____
Girish Ganjyal, Ph.D.

_____ Date: _____
Steven McGeehan, Ph.D.

_____ Date: _____
James E. Nelson, M.S.

Department Administrator: _____ Date: _____
Barbara Rasco, Ph.D.

ABSTRACT

The relative average degree of channelization (RADC) of starch granules may be important for identifying starch genotypes that are well-suited for chemical modification. The objective was to investigate development of a screening method for estimating RADC amongst starches of five maize inbred lines. Manual counting of channels within merbromin-stained starch granules visualized by confocal laser scanning microscopy was established as a RADC reference method, grouping starches of the five lines into high (Oh43), intermediate (A188, W22), and low (B73, W23) RADC categories. Total specific surface area values obtained by nitrogen gas adsorption were strongly correlated (0.92) to reference RADC rankings of the starch lines. However, fluorescent intensities of starch granules modified in a surface reaction with a fluorescent probe did not correlate with the reference rankings. Nitrogen gas adsorption represents a potential screening technique for estimating RADC, though furtdher refinement of the method is yet needed.

ACKNOWLEDGEMENTS

I would like to express my deeply gratitude to my major advisor, Dr. Kerry C. Huber, for all the advice, guidance, endless patience and encouragement that he has given me during the entire period of my study. This opportunity of learning from him and studying in his lab group is a precious experience for me. I would like to express my sincere thanks to my committee members, Dr. Girish Ganjyal, Dr. Steven McGeehan, and Mr. James E. Nelson, for contributing their valuable time, assistance, and suggestions to help me complete the study. I would like to particularly thank Dr. Andrzej Paszczynski for providing access to the fluorometer and for consultations. I would like to thank Kathy Hendrix for all the academic assistance and especially, for the friendship that she has given me. I would like to thank Ann Norton for her assistance and training to allow me to use her microscope facility. I thank my senior lab colleagues, Dr. Jong-Yea Kim, Dr. Jung-Sun Hong, and Dr. Chao-Feng Hsieh, for sharing their precious experiences and helping me in my lab experiments. Finally, I want to express my deepest gratitude to my parents, Jung-Hsiang Chao and Hsiu-Mei Weng, for always supporting, encouraging, and believing in me.

TABLE OF CONTENTS

LIST OF FIGURES

LIST OF TABLES

1.0. INTRODUCTION

Starch is an abundant polysaccharide that is utilized extensively in food and non-food industries due to its abundance, low cost, and broad range of functionalities (Schwartz and Whistler 2009). It is widely used as a stabilizer or modifier (e.g., thickener, colloidal stabilizer, gelling agent, water retention agent) to maintain texture and consistency (Singh et al. 2007; Singh et al. 2003). However, native starch possesses physicochemical limitations such as high viscosity at low solid levels, low shear resistance, thermal depolymerization, and high retrogradation tendency, all of which restrict its use and make it less ideal for some food and industrial applications (Huber and BeMiller 2010; Singh et al. 2007). Therefore, starch is frequently chemically and/or physically modified to tailor its physicochemical properties in accordance with the intended end use (Huber and BeMiller 2010). Upon modification, starch may exhibit enhanced functional properties including cold-water swellability and solubility; altered digestibility; improved paste clarity, flow properties, gel strength, freeze-thaw stability, and water-holding capacity; increased tolerance to pH, shear, and temperature stresses; and decreased susceptibility to retrogradation (Huber and BeMiller 2010). Starch chemical modification is generally achieved by cross-linking, substitution (i.e., etherification or esterification), oxidization, and/or acid or enzymatic hydrolysis (Singh et al. 2007), while physical modification is traditionally accomplished by varied combinations of heat and moisture treatments (Huber and BeMiller 2010; Jacobs and Delcour 1998; Singh et al. 2007). Starch chemical modification can be influenced by both extrinsic (i.e., conditions of reaction, nature of the reagent, reaction system components, etc.) and intrinsic (i.e., starch genotype, granule architecture and microstructure, presence of proteins, etc.) factors. To obtain a

modified starch with the desired functional properties, it is critical to select a suitable native starch source and an appropriate modification scheme (Singh et al. 2007).

Starch granule architectural features such as surface pores, channels, and connected internal cavities, have been shown to influence the flow of reagent into granules during starch chemical modification. These granule pores and channels provide a delivery path for reagent to access the granule interior and/or matrix and influence reaction patterns within modified starch granules (Huber and BeMiller 1997; Kim and Huber 2008). Given the influence of pores and channels in starch reactions, the ability to quantify the relative numbers of channels in a population of granules could be important for identifying starch lines or genotypes that may be best suited for chemical modification.

2.0. LITERATURE REVIEW

2.1. Molecular Structure of Starch

Starch consists of two primary macromolecules: amylose (AM) and amylopectin (AP). Depending on the ratio of amylose to amylopectin, a starch may be classified as normal (20-25% AM), high amylose (55-70% AM) (Ozturk and Koksel 2014), or waxy (≤ 5% AM) (Cano et al. 2014).

Amylose (Figure 1) is predominantly a linear polymer comprised of α-(1→4)-linked D-glucopyranose units (DP_n 600 – 6,000; M_w $1x10^5$ – $1x10^6$) (BeMiller and Huber 2012; Li et al. 2014; Tester et al. 2004; Xie et al. 2013), but may also possess a small degree of α-(1→6) branching depending on the botanical source (Buleon et al. 1998; Hoover 2001; Jacobs and Delcour 1998; Perez and Bertoft 2010; Tester et al. 2004). Conversely, amylopectin (Figure 1) is a much larger molecule (DP_n 9,600 - 15,900; M_w 1×10^7 - 1×10^9) (BeMiller and Huber 2012; Li et al. 2014; Tester et al. 2004; Xie et al. 2013), exhibiting a branch-on-branch structure, with branch points initiated via α-(1→6) linkages and linear branch chain segments being comprised of α-(1→4)-linked D-glucopyranose units (Buleon et al. 1998; Hoover 2001; Jenkins et al. 1993; Perez and Bertoft 2010; Tester et al. 2004). According to the "cluster" model, AP branch chains are not randomly distributed, but instead occur in clusters along AP internal chains (Hizukuri 1985; 1986). Within the cluster model, AP branch chains are further defined as A-, B-, or C-chains (Figure 2). A-chains are the short terminal chains, which themselves give rise to no further branched chains. B-chains possess one or more branch chains, and may be further sub-classified based on the number of clusters in which a given chain participates: namely B1 (limited to one cluster), B2 (spans two clusters), or B3 (spans

three clusters) chains. C-chains possess the lone reducing end of the AP molecule (Hizukuri 1986).

2.2. Granular Structure of Starch

Starch molecules, AM and AP, are biosynthesized and organized to form discrete semi-crystalline particles, termed granules. Depending on botanical source, these granules may vary in regard to both size (1 μm – 100 μm in diameter) and shape (disc, spherical, oval, polygonal, lenticular, elongated, kidney, etc.) (Buleon et al. 1998; Lindeboom et al. 2004; Perez and Bertoft 2010; Tester et al. 2004). When viewed under polarized light, native starch granules exhibit birefringence (i.e., a polarization cross), which is a characteristic of a radial arrangement of chains within granule crystalline regions (Tester et al. 2004). Optical and electron microscopy reveal that starch granules consist of layered alternating crystalline and amorphous concentric shells referred to as 'growth rings' (Figure 3 A), each of which possesses a thickness ranging from 100 to 400 nm depending on botanical source (Jenkins and Donald 1995; Perez and Bertoft 2010; Tester et al. 2004). These multi-layered concentric shells extend radially from the hilum to the outer surface of granules (Gallant et al. 1997; Jenkins et al. 1993; Tester et al. 2004), and become gradually thinner toward the granule periphery (Kossmann and Lloyd 2000).

Based on scanning electron microscopy (SEM) evidence, Gallant et al. (1997) proposed growth rings to be further comprised of spherical or ellipsoidal of blocklet structures (Figure 3 B). These blocklet structures are similar in shape, but vary in size, for the various botanical sources of starch. For example, blocklet size is reported to differ for pea (130 – 250 nm), wheat (25 – 100 nm), and corn (10 – 30 nm) starches (Perez and Bertoft 2010). A given

blocklet (Figure 3 C) is further comprised of alternating crystalline and amorphous lamellae (Figure 3 D), exhibiting a combined repeat distance of approximately 9 – 10 nm (Jenkins et al. 1993; Jenkins and Donald 1995). The crystalline lamellae consist of linear double helical segments of AP branch chain clusters, while the amorphous lamellae comprise the branching regions of AP chains (Figure 3 E) (Gallant et al. 1997; Jenkins et al. 1993; Jenkins and Donald 1995). AP chains are oriented with their reducing ends directed inward toward the granule hilum (Kossmann and Lloyd 2000).

Based on its susceptibility to acid hydrolysis within the granule, AM is proposed to exist within and/or traverse amorphous regions of starch granules (Robin et al. 1974), and has been suggested to be randomly situated between bundles of AP branch chain clusters within both crystalline and amorphous granule shells (Oates 1997). Jenkins and Donald (1995) theorized that AM may partially co-crystallize with AP chains on a limited basis, but likely contributes an overall disruptive influence to granule crystalline regions. In support of this concept, Yuryev et al. (2004) observed that an increase in amylose content correlated with a decreased difference in the electron density between the crystalline and amorphous regions of wheat starch granules, confirming a disruptive influence for AM chains within granule crystalline regions (Blazek and Gilbert 2011; Salman et al. 2009). AM may also exist in granules as a single chain, which may form amorphous inclusion complexes with suitable complexing agents (e.g., phospholipids, free fatty acids, etc.) (Hoover 2001; Perez and Bertoft 2010; Tester et al. 2004).

2.3. Microstructural Features of Starch: Pores and Channels

Fannon et al. (1992) reported the presence of surface pores (0.1 – 0.3 μm in diameter) at the external surfaces of corn, sorghum, and millet starch granules, and confirmed that these surface pores were true features of native starch granules, rather than artifacts of drying, enzymatic degradation, specimen preparation, or electron microscopy. Pores (Figure 4 A) were shown to be randomly distributed on the surfaces of maize, sorghum, and millet starch granules, and along the equatorial groove of large (i.e., A-type) granules of wheat, barley, rye, and triticale, with varying numbers of pores per granule (Fannon et al. 1992; Huber and BeMiller 2000; Naguleswaran et al. 2011). More recently, Kim and Huber (2008) observed pores originating from surfaces other than those of the equatorial groove region for wheat starch A-type granules. For maize starch granules, the frequency and number of pores per granule did not have any direct relationship with granule size, though pores were reported to often occur in clusters (Fannon et al. 1992). Fannon et al. (1992) did not observe surface pores on rice, oat, potato, tapioca, arrowroot, or canna starch granules via SEM. More recently, Sujka and Jamroz (2009) used atomic force microscopy (AFM) to examine the surface features of potato and corn starch granules. They observed no surface pores on potato starch granule surfaces, but reported pores of approximately 121 nm in diameter on the surfaces of corn starch granules. Juszczak et al. (2003b) utilizing non-contact AFM, reportedly observed different sizes and shapes of granular depressions, which were noted as possible surface pores on rice and oat starch granules, though the presence of surface pores on these granule types never has been further substantiated.

Initial evidence was presented by Fannon et al. (1993) that surface pores on corn and sorghum starch granules were openings to channels (0.07 – 0.1 μm in diameter), which

appeared to penetrate granules in a radial fashion. Huber and BeMiller (1997) provided the first conclusive evidence that starch granule pores were in fact openings to channels (Figure 4 B), many of which connected the external granule environment to the granule cavity or hilum region located at the approximate center of granules. Confocal laser scanning microscopy (CLSM) was used to demonstrate that channels penetrated granules to varying depths and that not all channels appeared to extend all the way to the granule cavity (Huber and BeMiller 2000). This evidence superseded the supposition of Gallant et al. (1997), who had proposed channels to be short, discrete protrusions into granule surfaces (extending at most a few growth rings inward) that were filled with amorphous starch material, rather than existing as a void or open space.

Oates (1997) suggested a possible origin for pores and channels in relation to the superhelical AP model proposed by Oostergetel and Vanbruggen (1993). In this model, segments of AP molecules were proposed to form a superhelical structure with a central void, which was estimated to be ~8 nm in diameter (Oostergetel and Vanbruggen 1993). However, the model proposed by Oostergetel and Vanbruggen (1993) was based on potato starch granules, which lack surface pores (Dhital et al. 2010; Fannon et al. 1992) and exhibit an exocorrosion (rather than an internal) digestion pattern in response to enzymatic treatment (Huber and BeMiller 2000; Oates 1997). Channels comprising the central voids of superhelicies (~8 nm in diameter) are much too small to be the pores and channels observed by Fannon et al. (1993) and Huber and BeMiller (1997).

2.4. Channel Structure and Composition

Starch granules possess trace levels of protein that are either bound to external surfaces (e.g., endosperm proteins) or embedded within the matrix (e.g., residual starch biosynthetic proteins) of granules; these proteins are commonly referred to as starch granule-associated proteins (SGAP) (Baldwin 2001). Han and Hamaker (2002) utilized a protein-specific probe, 3-(4-carboxybenzoyl)quinolone-2-carboxaldehyde (CBQCA) to investigate the locale of SGAP within granules. The utilized probe fluoresced only after reaction with primary amines, highlighting the location of SGAP within starch granules. In this investigation, starch granule channels were demonstrated to be lined with protein. In subsequent studies utilizing CLSM, the incidence of SGAP lining channels in maize starch granules was reduced after treatment with thermolysin (Figure 5), indicating that proteins within channels could be largely removed by protease treatment (Gray and BeMiller 2004; Han et al. 2005). Han et al. (2005) also identified the major protein missing after thermolysin treatment to be brittle-1 (*bt1*), a translocator of ADP-glucose into amyloplasts during starch biosynthesis.

Further, in addition to protein, phospholipids were shown to be present at channel surfaces in maize starch granules (Benmoussa et al. 2010; Lee and BeMiller 2008), with lysophosphatidylcholine identified as the primary phospholipid occurring in channels (Lee and BeMiller 2008). While the origin of channels has remained unclear for some time, Benmoussa et al. (2010) identified structural (actin-like and tubulin-like) proteins as constituents of maize starch granule channels, and further visualized filamentous structures or microtubules within developing maize endosperm amyloplasts by transmission electron microcopy (TEM). They proposed that channels could be the remnants of such microtubules,

which could have the role of facilitating delivery of substrate into developing starch granules during biosynthesis, as originally hypothesized by Fannon et al. (2004).

2.5. Influence of Channels on Reaction Patterns within Starch Granules

As pores were demonstrated to be openings to channels that connected the external and internal environments of granules (Gray and BeMiller 2004; Han et al. 2005; Huber and BeMiller 1997; 2000; 2001; Kim and Huber 2008), it was hypothesized that channels could provide a possible delivery path for reagent to access the granule interior and/or matrix during starch chemical modification reactions. Nevertheless, a certain degree of granule hydration/swelling was required for reagent to enter the granule matrix from either external granule or channel surfaces (Huber and BeMiller 1997; Kim and Huber 2008). A fluorescent probe, 5-(4,6-dichlorotriazinyl)aminofluorescein (DTAF), was used to investigate reaction patterns within wheat starch granules under both non-hydrated (starch non-swelling) and hydrated (starch swelling) conditions (Kim and Huber 2008). In non-hydrated starch reactions, DTAF labeling was limited to granule surfaces (including those of channels and cavities) (Figure 6 A), whereas starch granules reacted in a sufficiently hydrated state were derivatized by DTAF within the granule matrix (Figure 6 B). Thus, the degree of granular hydration/swelling appeared to greatly influence the flow of reagent into the granule matrix via channels. To simulate the path of reagent flow into the granule matrix in hydrated starch reactions, an intermediate degree of reagent infiltration into starch granules was achieved by limiting the length of infiltration time for dye to enter the granule matrix (Huber and BeMiller 2000). They concluded that channels within maize and sorghum starch granules represented a primary delivery path for reagent to access the granule matrix during reaction, and that

reagent entered the granule matrix from channels (lateral flow) and cavities (inside-out flow pattern from the granule hilum toward the periphery of granules) (Huber and BeMiller 2000).

In extending these initial findings to actual modification reactions, Huber and BeMiller (2001) demonstrated that phosphoryl chloride ($POCl_3$), a fast reacting reagent, reacted primarily at granular surfaces, including those of channels and cavities, and that channels and cavities represented a key path by which reagent entered the granule matrix. Thus, channels do influence reaction patterns within starch granules, and appear to enhance reaction homogeneity during starch modification.

More recently, Dhital et al. (2013) reported a high degree of structural heterogeneity among maize starch granules, based on diverse rates of diffusion observed among maize starch granules infiltrated by fluorescent dextran probes. Regardless of the size of the dextran probe or prior enzymatic treatment to enhance granule porosity, the diffusion rate of these probes into the granule matrix was categorized as either fast or slow for a given starch granule. A fast rate of diffusion was attributed to the ability of dextran probes to quickly access the granule central cavity via pores and channels, whereas a slow rate of diffusion was explained by a reduced capacity for probes to access the granule matrix. Dhital et al. (2013) suggested the granule matrix to be comprised of more densely packed bulk starch with much smaller voids (relative to those of pores and channels), presenting a more substantial barrier to the diffusion of fluorescent dextran probes.

2.6. Surface Area of Starch Granules

Surface structures of starch granules and porosity may not only be examined by microscopic techniques (Baldwin et al. 1998; Baldwin et al. 1997; Dhital et al. 2013; Fannon

et al. 1992; Fannon et al. 1993; Huber and BeMiller 1997; 2000; Juszczak et al. 2003a; b; Kim and Huber 2008; Naguleswaran et al. 2011; Sujka and Jamroz 2009), but also by the physical adsorption of gas or liquid by surface structures (Fortuna et al. 2000; Hellman and Melvin 1950; Juszczak et al. 2002; Kim and Huber 2010; Sujka and Jamroz 2009). A nitrogen gas adsorption technique has been used to evaluate starch granule surface characteristics and porosity in numerous studies (Sujka and Jamroz 2009). The surface porosity of starch granules is primarily described by a parameter termed specific surface area, which is defined as the total surface area of the porous solid per unit mass (m^2/g) (Klobes et al. 2006). This parameter accounts for those external surfaces that are available to adsorb gas or liquid molecules (Sujka and Jamroz 2007).

Using nitrogen gas adsorption, Hellman and Melvin (1950) reported specific surface area values for native starch granules of dasheen (2.62 m^2/g), corn (0.70 m^2/g), tapioca (0.28 m^2/g), and potato (0.11 m^2/g). Juszczak et al. (2002) measured specific surface area values for maize (0.687 m^2/g), waxy maize (0.675 m^2/g), wheat (0.534 m^2/g), triticale (0.383 m^2/g), barley (0.599 m^2/g), oat (1.244 m^2/g), and rice (1.267 m^2/g) starches. Further values determined by Sujka and Jamroz (2009) are 0.58 m^2/g for corn starch and 0.16 m^2/g for potato starch. In these aforementioned studies, reported specific surface area values for maize starch granules were in the range of 0.58 – 0.70 m^2/g. Though a nitrogen gas adsorption technique was common to all of these studies, observed experimental differences for a given starch botanical source were likely due to variations in experimental schemes and/or the varieties/cultivars analyzed.

In addition to nitrogen gas adsorption, Hellman and Melvin (1950) also measured specific surface area via a photomicrographic method, and reported values of 0.483 m^2/g and

0.152 m^2/g for corn and potato starches, respectively. While specific surface area values measured by both methods were similar for potato starch, the photomicrographic value for corn starch was noticeably lower than that (0.70 m^2/g) obtained by nitrogen gas adsorption. This difference has since been attributed to surface pores and channels, which are present on the surfaces of corn, but not potato, starch granules (Fannon et al. 1992; Kong et al. 2003).

Likewise, Soulaka and Morrison (1985) calculated mean volumes for wheat starch A- and B-type granules (based on particle size analysis) under the assumption that all granules are spherical. Their calculated specific surface value ranges for A- and B-type wheat starch granules were 0.236 - 0.302 m^2/g and 0.684 - 0.920 m^2/g, respectively. Employing a nitrogen gas adsorption technique, Kim and Huber (2010) determined the specific surface areas of soft wheat starch A- and B-type granules for waxy (0.86 and 2.76 m^2/g, respectively) and normal (0.76 and 2.33 m^2/g, respectively) lines. They further theorized that the slightly higher specific surface area values observed for waxy (as opposed to normal) wheat starch granules could reflect a difference in the extent of granule channelization and/or cavity dimensions (given that the average granule diameters for waxy and normal A- and B-type granules were virtually the same). Further, specific surface area values measured by gas adsorption were much higher than the calculations determined by Soulaka and Morrison (1985), which accounted for only external surfaces of A- and B-type granules. Thus, specific surface area measurements of starch granules measured via nitrogen gas adsorption would be expected to account not only for external surfaces of granules, but also internal granule surfaces of contributed by channels and connected cavities (Juszczak et al. 2002; Kim and Huber 2010).

2.7. Quantitation of Channel Frequency

Channels have a demonstrated role in facilitating the flow of chemical reagent into the starch granule interior, providing not only added access to interior surfaces for reactions, but also influencing granule reaction patterns by aiding the flow of reagent into the granule matrix. Given this documented role, the ability to quantify the relative number of channels in a population of granules could be important for identifying starch inbred lines or genotypes that are best suited for chemical modification. Widya et al. (2010) investigated development of a method to quantify the relative average degree of channelization (RADC) using a series of maize inbred lines believed to possess a range of pore/channel frequencies. These maize inbred lines were grown in the same field under common environmental conditions; therefore, potential differences in channel frequency were proposed to reflect differences in genetic make-up. The report of Widya et al. (2010) represents the sole attempt to date to quantify RADC within maize starch granules, and will be the focus of the ensuing discussion.

For assessing RADC, Widya et al. (2010) investigated a total of six different methods, each of which was based on one of three general approaches: 1) differential rates of amyloglucosidase digestion (based on the hypothesis that granules with greater channel frequencies would be hydrolyzed more rapidly than those with lower channel frequencies); 2) direct counting of pores at granule surfaces (given that pores are openings to channels); and 3) quantitation of total channel proteins or a specific channel protein (given that the amount of total channel protein or the quantity of a specific channel protein could reflect the degree of channelization, based on its known association with channel structures).

Differential Rates of Amyloglucosidase Digestion. This approach of Widya et al. (2010) assumed that the average surface areas of individual starch granule channels and cavities were

equal across all maize inbred lines. However, light microscopy evidence has revealed that *su2* mutant starch granules have relatively large channels, whereas the *wx* mutant has comparatively large granule cavities, comprising almost 50 % of the total granule cross section. Thus, the assumption that granule channels and cavities of various maize lines have standard or common dimensions may not be completely valid. Further, the different enzymatic digestibilities of maize lines may not strictly be the result of a greater or lesser channel frequency, but could be due to other structural factors such as amylose content or crystalline packing arrangement, neither of which were verified in this study. Though a correlation between channel frequency determined by enzymatic digestion and rate of amyloglucosidase digestion was somewhat apparent, the relationship was not linear. In conclusion, the amyloglucosidase digestion rate of maize starch granules was likely affected by factors other than channel frequency, and was not been fully validated for estimating RADC (Widya et al. 2010).

Direct Counting of Pores. Numbers of granule surface pores were manually counted in SEM micrographs in attempt to obtain actual RADC values for starches of inbred maize lines. This initial method proved difficult, as it was not always straightforward to distinguish small pores from other granule surface features. To aid visualization of surface pores, starch granules were treated with α-amylase (either with or without prior thermolysin treatment to remove channel proteins) for the purpose of enlarging surface pores to make them more visible for counting. However, amylase treatment resulted in either the formation of surface grooves or a high degree of surface exo-corrosion for some granules, making it impossible to accurately identify and count numbers of individual pores. Widya et al. (2010) concluded that this latter method significantly underestimated actual numbers of surface pores, and was

adversely impacted by the heterogeneous effects of α-amylase treatment on surface pore size and shape for granules of the maize inbred maize lines, confounding determination of channel frequency.

Quantitation of Channel Proteins. Protein methods investigated for estimating RADC included quantification of total channel proteins (31 – 97.4 kDa), a specific channel marker protein (≈42 kDa), or actin. All three approaches commonly identified two lines estimated to possess the highest and second highest RADC values (
Table 1), as well as the line estimated to possess the lowest RADC value (lines estimated to possess intermediate RADC values were not consistently ranked by the three methods). Given that it was impossible to completely remove external granule surface proteins prior to extracting channel proteins (and because total channel protein compositions differed among inbred maize lines), it was hypothesized that an approach utilizing a specific channel protein marker (i.e., 42 kDa protein or actin) may provide the most accurate estimation of RADC. The channel marker protein (≈42 kDa) was observed to be present in the total channel protein extracts of every maize inbred line. The method measuring the quantity of actin in channel protein extracts was based on the concept that channels are remnants of amyloplast microtubules and thus, are a potential indicator of channel frequency. Of the two methods focusing on a sub-component (i.e., 42 kDa protein or actin) of the channel protein extract, Widya et al. (2010) identified the actin approach as the preferred method of choice given that it was straightforward to conduct, reproducible, and required only a minute amount of starch (2-3 corn kernels was sufficient).

In summary, the research conducted by Widya et al. (2010) represents a valuable contribution that enhances ability to identify and screen various maize starches in regard to

channel frequency. Nevertheless, while all three protein-based approaches provided fairly similar estimations of RADC (Widya et al. 2010), observed inconsistencies in RADC rankings among these three methods make it difficult to unequivocally identify a single method that best estimates relative channel frequency. This problem is further compounded by the lack of an objective reference method capable of establishing actual RADC values for the evaluated maize lines. In short, there is further need not only to explore additional experimental methods for estimating RADC, but also for the establishment of an objective method capable of quantifying relative numbers of channels within starch granule populations.

3.0. OBJECTIVES

The overall goal of this research was to investigate the development of a simplified method to efficiently and effectively quantify the relative average degrees of channelization (RADC) amongst maize starch granule populations of five maize inbred lines.

Specific Objectives

1. Validate the presence of surface pores and channels within maize starch granule populations, and establish a relative ranking of the five maize lines in regard to RADC for use as a reference in subsequent method development.
2. Evaluate simplified approaches for quantifying RADC within the five distinct maize starch granule populations.
3. Determine the extent to which simplified methods (objective 2) predict RADC relative to the established reference rankings (Objective 1).

4.0. MATERIALS AND METHODS

4.1. Maize Inbred Lines

Five maize inbred lines, A188, B73, Oh43, W22, and W23, were graciously provided by Dr. James N. BeMiller of the Whistler Center for Carbohydrate Research (Purdue University, West Lafayette, IN) from the collection of Dr. David V. Glover. Starch was isolated from whole maize kernels following the method described by Wongsagonsup et al. (2008) and Sui et al. (2011). Maize starch granules of each line were passed over a 106 μm sieve (No. 140, S/N 061195522, metric, 0.0041 inches, Fisher Scientific Co.) to exclude any large particles of aggregated granules or kernel constituents prior to derivatization.

4.2. Scanning Electron Microscopy (SEM)

Surface pores amongst the five maize starch granule populations were visualized by scanning electron microscopy (SUPPA^{TM} 35VP, Carl Zeiss Microimaging Inc, Thornwood, NY) according to parameters described by Kim and Huber (2008). Starch granules were mounted onto aluminum stubs using double-sided carbon tape, coated with 20 nm gold-palladium (60:40), and visualized at an accelerating voltage of 3 - 6 kV.

4.3. Starch Granule Size Distribution

Granule size distributions for the five maize inbred lines were determined similar to the method of Geera et al. (2006) using an Accusizer 780 equipped with SW 788 software for Windows (Particle Sizing Systems, Santa Barbara, CA, USA). Individual particles were detected in the range of 0.6 – 400 μm.

More specifically, the instrument was first standardized by uploading calibration files provided by the instrument manufacturer in preparation for analysis. Deionized water was used as a blank to ensure that the maximum number of detected particles for a blank did not exceed 2,000/ml. In the event that this threshold was reached, the system was flushed with fresh deionized water (25 ml) four times and re-measured to ensure that it fell within the acceptable limit. The analysis of a starch sample was conducted by injecting a sufficiently diluted starch suspension (0.002 – 0.004 g starch in 350 ml deionized water) into the instrument, such that granules passed only one at a time through the instrument sensing zone, thus avoiding multi-granule sensing coincidences. Appropriate sample dilution was monitored by ensuring that the maximum number of detected particles for a given injection fell between 6,000 – 9,000 (based on the protocol suggested by the instrument manufacturer and preliminary studies using starch samples). The background signal for the blank was then subtracted from that of each respective starch granule size distribution profile. Between measurements of different starch samples, the system was flushed four times with deionized water (25 ml/per flush) to prevent cross-contamination. System software computed starch granule size distributions on the basis of both number percent (%) and volume percent (%), with the latter was also being converted to weight percent (%) presuming a spherical shape and a hydrated starch density value of 1.40 g/ml (Soulaka and Morrison 1985).

4.4. Merbromin Treatment of Starch Granules

Maize starch granules were stained with a methanolic solution of merbromin as described by Kim and Huber (2008) for visualization of granule channels and cavities.

Treated granules were subsequently visualized via confocal laser scanning microscopy as described below (section 4.5).

4.5. Confocal Laser Scanning Microscopy (CLSM)

Merbromin-treated maize starch granules were visualized via confocal laser scanning microscopy (Olympus Fluoview 1000 system, Olympus America Inc., Center Valley, PA, USA) equipped with an upright Olympus BX61 microscope. Starch granules were evenly dusted onto a glass slide that had been lightly coated with paraffin wax, after which the slide was passed twice quickly over a flame to affix starch granules. A drop of immersion oil and a glass cover slip were added to the slide, and after which another drop of immersion oil was added to top of the cover slip prior to observation with a 60x oil objective lens. Excitation was achieved with a 488 nm laser (solid state) operated at 6% power, while emission was collected in the 500-600 nm range. For image acquisition, scan speed (12.5 µsec/pixel), frame size (1024x1024 pixel, 12 bits pixel depth), optical zoom (1.0x), and optical section thickness (0.37 µm) were held constant for all treated starches of each starch inbred line. Five consecutive optical cross-sections representing the approximate geometric centers of granules were digitally stacked together on the z-axis using Olympus FV10-ASW Viewer software (Olympus, Richmond Hill, Ontario, Canada) to reveal the inner features of the granule matrix.

4.6. Manual Counting of Channels from CLSM Images

Criteria were established to manually count the numbers of channels (highlighted by merbromin fluorescent dye) within individual starch granules of CLSM stacked images to calculate the relative average degree of channelization (RADC) for each inbred line. More

than 400 granules were counted for each maize inbred line, and mean RADC values were calculated across all counted granules for each respective line. The approximate geometric center of each granule included in the counting exercise was determined based on the clear observation of the granule cavity or hilum. For granules in which no cavity could be observed, the five optical cross-sections that resulted in the greatest granule diameter were used to create stacked images that best approximated the granule geometric center. Those granules that fell at the edge of an optical field (i.e., only a portion of the granule was visible) or that did not yield sufficient optical cross-sections within the inner regions of the granule matrix (i.e., granules that were above or below the primary imaging plane) were not included in the channel counting exercise.

Within selected stacks of optical cross-sections, countable channels occurred in multiple forms including bright dots (i.e., channels that protruded directly away from the viewer), entire or partial segments of serpentine lines within the granule matrix, and/or clusters of channels at the granule periphery (Huber and BeMiller 1997; 2000). In first two scenarios, the possibility existed for two (or more) channels originating from different point of the granules periphery to later intersect (i.e., become a single channel) further into the granule matrix. Nevertheless, no effort was made to account for this possibility (was not always possible or practical to so so); thus, distinct segments of channels that originated from different points of the granule periphery were counted as separate and distinct channels. For the latter scenario, granule surface pores and channels often occurred in clusters at or near granule surfaces (Fannon et al. 1992), making it difficult to distinguish and count individual channels within stacks of multiple overlaid sections (Figure 7 A). In such cases, a single optical cross-section (usually the middle one within a given stack) was referenced to better distinguish individual

channels and more accurately count numbers of channels within these granules (Figure 7 B). This approach would possibly lead to a slight undercounting of channels, since a single optical cross-section was used and a channel was only counted if it could be determined to be distinct and separate from another. However, the approach allowed granules possessing high frequencies of channels to be counted and to not be eliminated from RADC calculations.

A granule in which only a highlighted cavity was observed, without the direct visualization of channels, was excluded from RADC calculations rather than counting the granule to possess zero channels. It was presumed that this type of granule possessed at least one channel, given the presence of dye at the cavity or hilum (Huber and BeMiller 2000). Since the number of channels could not be directly counted in this circumstance, such granules were excluded from RADC calculations. For a granule to possess zero channels, it had to exhibit the lack of both a dye-highlighted cavity and observable channels.

Small starch granules (< 5 μm) were especially problematic for counting channels. Given that the thickness (0.37 μm) of individual optical cross-sections was held constant, a stack of five optical cross-sections often encompassed an entire granule or a large portion of the external granule surface, which obscured visualization of the interior regions of granules (due to the high proportion of fluorescent dye adsorbed at the granule surface). Thus, detailed features within granules of this size were difficult to visualize using stacked cross-sections. However, even if a single optical cross-section was viewed, the interior features of these granules were still difficult to ascertain. Where a cavity or the hilum region of a granule could not be distinguished from that of the granule external surface, such granules were excluded from RADC calculations.

Granules that exhibited abnormal morphologies (i.e., broken or compromised granules) were also excluded from RADC calculations. For these granules, fluorescent dye was generally able to infiltrate the granule matrix (rather than being limited to granule surfaces), making it impossible to accurately distinguish internal features.

4.7. Specific Surface Area Measurement via Gas Adsorption

Starch granule specific surface area values for the five maize inbred lines were measured as described by Kim and Huber (2010) with minor modification. Starch was weighed into a sample tube prior to degassing, and was dried overnight at 120 °C under inert conditions using a Flowprep 060 degassing unit (Micrometrics, Norcross, GA, USA). Samples were weighed again after degassing, after which the specimen mass was determined prior to analysis of specific surface area. A Tristar 3000 Surface Area Analyzer (Micrometrics, Norcross, GA, USA) operated at liquid nitrogen temperature (77.3 K) was utilized for this analysis. Specific surface area of a starch sample was determined from the obtained adsorption isotherm, which yielded a mean value. Measurements for each maize inbred line were conducted in triplicate.

4.8. Surface Derivatization of Starch with a Fluorescent Probe

Starch of each of the five maize inbred lines was surface-derivatized with DTAF according to the procedure of Kim and Huber (2008) with minor modification. The procedure, which utilizes a triethylamine-chloroform reaction system, limits reaction to all exposed external surfaces of granules, including those of channels and connected cavities (Huber and BeMiller 2001; Kim and Huber 2008). Starch (1.0 g, dry basis [d.b.]) was suspended in

triethylamine (18 ml) within a round bottom flask (50 ml) with continuous vigorous stirring (30 min), after which chloroform (15 ml) was added to the suspension with continued stirring (10 min). Derivatization was subsequently initiated by addition of 200 µl of DTAF stock solution (20 mg DTAF in 2 ml DMSO) to the reaction system. Reaction was allowed to proceed at ambient temperature for 24 hr in the dark (to minimize photobleaching of DTAF) with sufficient stirring to prevent aggregation of starch granules. Following reaction, derivatized starch granules were collected by centrifugation (3000 g, 20 min). For removal of unreacted dye, derivatized starch granules were suspended in absolute ethanol (40 ml, 30 min) using a Wrist Action® Shaker (Burrel Scientific, Model 75, Pittsburg, PA, USA), after which the suspension was centrifuged (3000 g, 20 min), and the colored supernatant (containing unbound DTAF dye) was discarded. This ethanol washing procedure was repeated (a minimum four times) or until a colorless supernatant was obtained (indicating unbound DTAF dye had been removed). Washed starch granules were recovered by vacuum filtration on a Büchner funnel, allowed to air-dry overnight in the dark, and stored at 4 °C (in the dark) until further analyzed.

4.9. Microwave Dissolution of Derivatized Starch

DTAF-derivatized starches were solubilized according to the microwave dissolution method described by Kim and Huber (2006) with slight modification. Starch (100 mg, d.b.) was suspended in 90% dimethyl sulfoxide (DMSO, 10 ml) in a 60 mL Teflon-PFA jar (Savillex, Minneapolis, MN), and heated for 35 seconds in a microwave oven (R-303TKC, Sharp Electronics CORP., Mahwah, NJ, USA). After heating, the starch dispersion was gently shaken to facilitate complete dispersion of the starch within the container. The starch solution

was then held in the dark until it cooled to ambient temperature, after which it was subjected to fluorescence measurement.

4.10. Fluorescence Measurement of Solubilized DTAF Starch Derivatives

Fluorescence intensity of the solubilized DTAF starch derivatives was measured using a FluoroMax-3 Spectrofluorometer (Jobin Yvon Inc., Fdison, NJ, USA) equipped with a xenon lamp. Fluorescence intensity was determined using an excitation wavelength of 495 nm, while emission was collected over the range of 510 nm to 700 nm (at 1 nm intervals). Both the excitation and emission slit widths were held constant at 5 nm, while measurements were conducted at ambient temperature within a 10 mm glass cuvette (3-G-10, Starna Cells, Atascadero, CA). Each sample was set in the sample chamber in the dark for 7 min before fluorescence was measured.

4.11. Experimental Design and Statistical Analysis

Significant differences between the five maize inbred populations in regard to RADC (i.e., channel counting), gas adsorption, granules size, and fluorescent intensity were assessed using Analysis of Variance ($\alpha = 0.05$), while a least significant difference (LSD) test was used to differentiate treatment mean values ($P < 0.05$). Pearson's correlation analysis was conducted to investigate possible relationships amongst RADC measures and starch characteristics. All statistical computations and analyses were conducted using the Statistical Analysis System (SAS) for Windows (SAS Institute, Cary, NC, USA).

5.0. RESULTS AND DISCUSSION

5.1. Morphological Characteristics of Starch Granules of Maize Inbred Lines

Granule size distribution profiles (volume % basis) for the five maize inbred lines ranged from 3 – 36 µm, comparable to the literature-reported range of 2 – 30 µm (BeMiller and Huber 2012; Naguleswaran et al. 2012; Perez and Bertoft 2010; Tester et al. 2004). Maize starch granules of this study were isolated from kernels utilizing a laboratory procedure designed to retain native granule components (e.g., surface proteins). The upper 36 µm diameter cutoff of this study was experimentally determined, and appeared to represent the boundary between the largest individual starch granules and the relatively fewer larger particles likely comprising aggregates of granules, fiber, or other residual kernel materials. While each individual maize starch granule is generally synthesized within a separate amyloplast, a minority of amyloplasts may contain multiple granules, making these granules more difficult to isolate from plant tissue (Perez and Bertoft 2010). Such occurrences could account in part for the presence of occasional granule aggregates or particles larger than the 36 µm cutoff.

Granule size measurements utilizing particle sensing instruments generally calculate average granule diameters based on the assumption of a spherical shape (Lindeboom et al. 2004). Average starch granule diameters for the five maize inbred lines ranged from 14.38 to 16.80 µm (Table 2), and could be statistically differentiated into three groups (B73, W22 > A188 > W23, Oh43). However, the granule size distribution profiles for all maize populations were largely overlapped, indicating only minimal shifts in granule diameter profiles for the maize inbred lines.

Specific surface area values (m^2/g) for starch granules were calculated from the particle size profiles using a hydrated starch density value of 1.40 g/ml (Soulaka and Morrison 1985). Calculated specific surface area values for the five maize inbred lines ranged from 0.2762 – 0.3150 m^2/g (Table 2), and followed the order: Oh43, W23 > A188 > W22, B73, the exact reverse order of that obtained for average granule diameters. This inverse relationship between the two measurements was expected, since smaller diameter particles contribute a greater collective surface area than larger diameter particles for a given weight of starch. Further, calculated specific surface area values reported here accounted for only external surfaces of starch granules (as opposed to potential internal surfaces that would be contributed by channels and cavities). Thus, internal specific surface areas contributed by channels and cavities were not reflected in these estimations.

Based on microscopic observation, maize granule shape was observed to be polygonal, but approximately spherical. Pores were confirmed at the surfaces of granules for all five maize inbred lines via SEM. A scanning electron micrograph of granules isolated from the A188 maize inbred line is shown in Figure 8, and is representative of the appearance of native starch granules of the five maize inbred lines. Red arrows in the micrograph indicate a surface pore or a cluster of pores. Regardless of the size and shape of the starch granules, the number of visible surface pores differed from granule to granule for a given inbred line, as has been previously noted others (Fannon et al. 1992; Huber and BeMiller 1997; Kim and Huber 2008; Naguleswaran et al. 2011). Given the confirmed presence of surface pores on granules of all five maize inbred lines, it was presumed that granules of all lines also possessed channels. Thus, the starch granules of the five maize inbred lines were deemed to be suitable starch materials for further investigation of RADC.

5.2. Reference Ranking of RADC via Manual Channel Counting

Though the number of surface pores is likely indicative of the number of channels within a starch granule, the counting of individual pores was previously demonstrated to be highly problematic and unreliable due to the difficulty of visualizing and distinguishing the presence of very small pores on individual granules of SEM micrographs (Widya et al. 2010). An alternative approach utilized in this study was to directly count the numbers of channels, which had been first highlighted by a fluorescent dye, using CLSM images. Merbromin, a fluorescent dye (molecular weight 750.65 g/mole), has been shown to adsorb at granule surfaces, including those of channels, under starch non-swelling conditions without entering the granule matrix (Huber and BeMiller 1997). CLSM examination of merbromin-stained starches showed the presence of highlighted granule channels, cavities, and external surfaces. However, the high intensity of fluorescent signal at granule external surfaces made it difficult to clearly resolve individual channel features within the granules (Figure 9 A).

To better visualize channels for counting purposes, a stack of five optical cross-sections representing the approximate geometric center (excluding sections comprising external surfaces) of each granule was selected to construct a digitally-stacked image. The thickness (0.37 μm) of each optical cross-section and the number of cross-sections comprising a digitally-stacked image were held constant to ensure that numbers of channels were not over- or underestimated due to variable image parameters. Channel counting was conducted using digitally-stacked images representing the approximate geometric center of granules, allowing individual channel features to be more clearly visualized (Figure 9 B). However, the counting exercises described here did not yield absolute numbers of channels per granule, since not all regions of a given granule were represented in a given set of digitally-stacked images. Rather,

a channel count for a given granule reflected only the number of countable channels within a particular image stack. Thus, the channels counts depicted here reflect relative numbers of channels per granule or maize line, referred to as RADC.

Relative average degrees of channelization for starch granules of each of the five inbred maize lines are presented in Table 2, with the overall statistical ranking from highest to lowest following the order: Oh43 > A188, W22 > W23, B73. Therefore, from a statistical perspective, the starches of the five inbred maize lines could be classified into groups of high (Oh43), intermediate (A188 and W22), and low (W23 and B73) relative average degrees of channelization.

It was also interesting to note that the numbers of granules excluded from channel counting – due to the presence of a highlighted cavity, but the lack of any countable channels (Table 3) – followed the exact reverse order of the non-statistical, numerical ranking of inbred maize lines with respect to increasing levels of RADC (Table 2). The presence of a highlighted cavity within a granule would suggest the presence of at least one channel, by which the dye was able to access the hilum or cavity region of that particular granule. In this scenario, the likely reason a channel might not have been directly visualized was because it occurred in a region of the granule not included within the selected image stack of optical cross-sections. For a starch with a relatively low RADC, the probability of observing a channel within the selected stack of optical cross-sections of a given granule would be less than that for a starch with a relatively high RADC. Thus, the number of granules that would be excluded from counting for this reason would be expected to greater for an inbred line having a low RADC. This observed inverse relationship between the number of excluded granules (highlighted cavity – but no visible channels) and RADC ranking would offer some

credibility to the manual counting method. Further, as illustrated previously, the channel counting method also provided a reasonable statistical differentiation of the starches of the five maize inbred lines with respect to RADC. Lastly, given that the channel counting method provided a direct measure of channel frequency, it could ideally serve as an effective reference method. Thus, though labor-intensive and tedious, channel counting would appear to be represent a valid reference against which other potential RADC methods could be corroborated or validated.

5.3. Specific Surface Areas of Starch Granules of the Maize Inbred Lines

Hellman and Melvin (1950) and Soulaka and Morrison (1985) used indirect methods to calculate specific surface area values (derived from particle size data) for maize (0.483 m^2/g) and wheat (A-type 0.236 – 0.302 m^2/g, B-type 0.684 – 0.920 m^2/g) starch granules, respectively. The same parameter measured via nitrogen gas adsorption for starch granules of both maize (0.70 m^2/g) (Hellman and Melvin 1950) and wheat (waxy A-type 0.86 m^2/g, B-type 2.76 m^2/g; normal A-type 0.76 m^2/g, B-type 2.33 m^2/g) (Kim and Huber 2010) was noticeably higher than that obtained by simple calculation. Specific surface area values estimated by indirect methods accounted only for granule external surfaces, while those measured by nitrogen gas adsorption method reflected both external and internal (i.e., channel and cavity) surfaces of starch granules (Juszczak et al. 2002; Kim and Huber 2010). Thus, the observed differential between the two methods could provide a potential measure of the granule surface area contributed by internal structures such as channels and cavities. Thus, total specific surface area determined by nitrogen gas adsorption was deemed to represent a simple and straightforward approach for estimating RADC of starches.

Mean total specific surface area values for starches of the five maize inbred lines are shown in Table 2. Among the five lines, Oh43 starch granules statistically possessed a higher specific surface area value than the other four lines, suggesting a higher RADC for these granules. This result was also in general agreement with that obtained by the manual counting method. The simple ranking of granule specific surface area mean values of the five maize inbred lines from the highest to the lowest without reference to statistical significance followed the trend: Oh43 > A188 > W22 > B73 > W23, which trend was almost identical to that observed for the manual channel counting method (Oh43 > A188 > W22 > W23 > B73), except that the order of lines ranked in the fourth and fifth positions was reversed. A strong positive correlation was observed between total specific surface area (gas adsorption) and RADC estimated by manual channel counting (Table 4), suggesting that the total specific surface area measurement was indicative of the relative numbers of channels for a given starch. While the manual counting and gas adsorption methods were similar predictors of RADC, the experimental reproducibility and thus, statistical power, was much greater for the manual counting method. Further, total specific surface area determined by gas adsorption was not significantly correlated with granule morphological parameters (granule size, external granule specific surface area) (Table 4), providing evidence that specific surface area values contributed by channels and cavities (internal specific surface area) did not simply mirror those of external granule parameters. The fact that total specific area measurements, which reflect both external and internal surface areas, was strongly correlated to RADC determined by channel counting (but not external granule parameters) would suggest that the amount of surface area contributed by channels and cavities generally exceeds that of external granule surfaces.

In comparing measured specific surface area mean values for the five maize inbred lines with literature reported values for maize starch, the values obtained in this study were much (10-fold) greater (Table 2). Literature specific surface area values for maize starch measured via nitrogen gas adsorption have generally ranged from 0.58 – 0.70 m^2/g (Hellman and Melvin 1950; Juszczak et al. 2002; Sujka and Jamroz 2007; 2009), depending on the degassing conditions used. Degassing in these studies was generally accomplished by drying the starch samples in the range of 35 – 105 °C prior to analysis (Hellman and Melvin 1950; Juszczak et al. 2002; Sujka and Jamroz 2007; 2009). Given the discrepancy between literature-reported values and those of this study, it was theorized that observed differences might be caused by the relatively higher degassing temperature (120 °C) used in our study. To test this possibility, starches of maize inbred lines W22 and W23 were degassed at temperatures of 40 °C and 90 °C prior to analysis. Specific surface area values (Table 5) obtained from the three different degassing temperatures (40, 90, 120 °C) increased with increasing degassing temperature, with the largest incremental increase observed between 90 and 120 °C. Thus, the higher than expected total specific surface area values obtained for starches of the five maize inbred lines in our study appeared to be largely explained by differences in experimental protocol.

The estimation of specific surface area of a porous material by gas adsorption is determined by the sample adsorption isotherm of high purity liquid nitrogen. Prior to analysis, the removal of adsorbed contaminants (i.e., moisture and/or gas from the atmosphere) from the surface of the test material is accomplished to obtain an accurate result. Thus, a higher degassing temperature would be expected to produce a greater loss of moisture from the starch, and consequently, generate a higher starch specific surface area value as nitrogen gas

is adsorbed at available surfaces. The degassing temperature needed to achieve proper removal of surface contaminants without adversely affecting the sample depends on the nature of the material (Klobes et al. 2006). Given the wide range of degassing conditions noted in the literature for starch, further experiments are yet needed to establish the most appropriate degassing conditions that ultimately reflect absolute values of starch specific surface area. In short, while the specific surface area measurements generated in this study do not reflect absolute values, the relative differences observed amongst the five inbred maize starch lines can still potentially reflect differences in RADC. However, the precision associated with gas adsorption measurements could also be studied and improved to allow for greater differentiation of starch RADC by this method.

5.4. Surface Reaction of Starch Granules of the Maize Inbred Lines

Surface derivatization of starch granules with DTAF, a fluorescent probe, was investigated as a possible means for estimating starch RADC for the five maize inbred lines. DTAF forms covalent bonds with amino and thiol groups of proteins at ambient temperature and with hydroxyl groups of polysaccharides or proteins above pH 9 (Kim and Huber 2008; Schumann and Rentsch 1998; Siegler et al. 1989). Given that starch granule channels are lined with minor amounts of proteins and phospholipids (Han et al. 2005; Han and Hamaker 2002; Lee and BeMiller 2008), and are primarily comprised of starch chains, these granule surfaces represent ideal reaction sites for DTAF derivatization. Under non-aqueous reaction conditions (i.e., starch non-swelling conditions), DTAF reaction was shown to be limited to exposed starch granule surfaces, including those of channels and cavities; reaction did not occur within the granule matrix (Kim and Huber 2008). Thus, the proportion of fluorescence

intensity associated with starch granules after DTAF surface reaction was investigated as a possible means for estimating RADC of the five maize inbred lines.

Fluorescent spectra of the DTAF-derivatized maize starch samples (Figure 10) exhibited a similar band shape and maximum emission wavelength in the range of 537 – 539 nm. The emission maximum for DTAF is reported to be 516 - 517 nm (Ahmed et al. 2011; Schumann and Rentsch 1998; Siegler et al. 1989), though it may shift depending on solvent type. A shift to a higher maximum emission wavelength was reported for DTAF with an increase in solvent polarity (Aranda et al. 2012). Mean fluorescent intensities for DTAF-derivatized maize starches fell between 11.16×10^6 - 16.28×10^6 (Table 2). The overall ranking of mean fluorescence intensity (without statistical consideration) for the five inbred lines followed the order: A188 > Oh43 > B73 > W23 > W22. Maize inbred line A188 exhibited the highest fluorescent intensity among the five inbred lines, while Oh43 was the second highest (Table 2). Similar to gas adsorption, no correlation was observed between RADC estimated by fluorescent intensity and granule morphological parameters, suggesting that fluorescence intensity was not simply related to the extent of DTAF reaction at external granule surfaces. However, RADC estimated by DTAF fluorescent intensity also showed no strong correlation with RADC determined via either manual channel counting or gas adsorption (Table 4). The absence of a correlation between DTAF fluorescence intensity and other RADC methods (i.e., channel counting, total surface area by gas adsorption) would suggest that factors other than total surface area influenced the extent of DTAF reaction at granule surfaces.

Though gas adsorption and DTAF surface reaction methods both involved physical sorption of nitrogen gas or covalent bonding of fluorescent probe molecules at available granules surfaces, the reaction of DTAF necessitated chemical bonding to specific functional

groups of starch, protein, or lysophospholipid molecules comprising granule surfaces. Sui and BeMiller (2013) derivatized starches of maize inbred lines, categorized into groups of either high or low RADC, with both rapid and slow reacting chemical reagents. They observed that the extent of derivatization did not exactly follow the RADC trend, and suggested that other starch intrinsic factors on a granular and/or molecular level (other than RADC) predominantly impacted the reactivity of the starches of the maize lines. Thus, it is likely that differences in starch intrinsic factors amongst the five maize inbred lines influenced the extent of the DTAF reaction, explaining the lack of agreement between the DTAF and channel counting/gas adsorption RADC methods. Nevertheless, the DTAF surface reaction method did effectively identify maize inbred lines A188 and Oh43 to exhibit a relatively high RADC, though the exact order the RADC rankings were not consistent with the other two noted methods. Thus, the DTAF fluorescent probe method could still have some potential utility as a coarse screening tool for identifying starch genotypes with relatively high RADC.

5.5. Comparison of RADC Rankings Established Two Different Studies

RADC rankings of the five maize inbred lines established in this study via channel counting, nitrogen gas adsorption, and DTAF surface reaction methods were compared with those published by Widya et al. (2010), involving quantitation of channel proteins (Table 6). Maize inbred line Oh43 was determined to possess the greatest RADC by all methods, except for the DTAF fluorescent probe method (in which Oh43 was ranked 2nd highest). With the exception of the DTAF fluorescent probe method, B73 was consistently observed to have either the lowest or the second lowest RADC by all other methods. Line W22 showed intermediate RADC by most methods, with exception of slightly lower RADC ranking by

actin protein and DTAF methods. Thus, RADC rankings of Oh43, W22, and B73 maize inbred lines were generally similar across five of the RADC methods, and may be grouped into high (Oh43), intermediate (W22), and low (B73) RADC categories. In contrast, RADC rankings for maize inbred lines A188 and W23 were the exactly reversed for the channel counting method of this study and the total channel protein and 42 kDa protein methods of Widya et al. (2010) (Table 6). Due to this discrepancy, no significant correlations were found between RADC methods of this study and those of Widya et al. (2010) (Table 7), though significant correlations were noted between evaluated methods within each of the two studies. Possible explanations for this discrepancy could be that the starch samples utilized in the two studies were isolated from kernels of two different crop years (i.e., an environmental effect), an inadvertent mislabeling of starch samples in one of the two studies, or simply that the methods of the two studies simply disagree.

6.0. SUMMARY AND CONCLUSIONS

Starches of the five maize inbred lines were categorized into levels of high (Oh43), intermediate (A188 and W22), and low (W23 and B73) RADC according to the results of the manually channel counting reference method, which was theorized to provide the most accurate estimation of RADC in this study. Though this method was the only one to involve direct counting of channels, it was extremely labor-intensive and thus, is not generally appropriate for routine screening of starches for RADC. Nevertheless, the determination of starch total specific surface area by gas adsorption was highly correlated ($r = 0.92$) with the manual counting method with respect to RADC, though its capacity to statistically differentiate starches of the maize inbred lines into distinct RADC categories was less efficient. Further, starch total surface area determinations by gas adsorption were highly dependent on degassing conditions, and provided only relative measures of starch total surface area. Additional study is yet needed to identify a degassing protocol that provides the most accurate estimation of actual or absolute starch total surface area. The DTAF method, in which starch granule surfaces (including those of channels and cavities) were derivatized with a fluorescent probe, did not correlate well with either the manual counting or gas adsorption methods. This method appeared to provide the least reliable RADC rankings, as intrinsic factors of the starches themselves appeared to influence reactivity aside from RADC.

In comparing RADC rankings of the five maize inbred lines established in this study with those determined by Widya et al. (2010), RADC rankings for three of the five maize inbred lines were in general agreement. In light of the findings of both studies, three maize inbred lines may be effectively classified into high (Oh43), intermediate (W22), and low (B73) RADC categories.

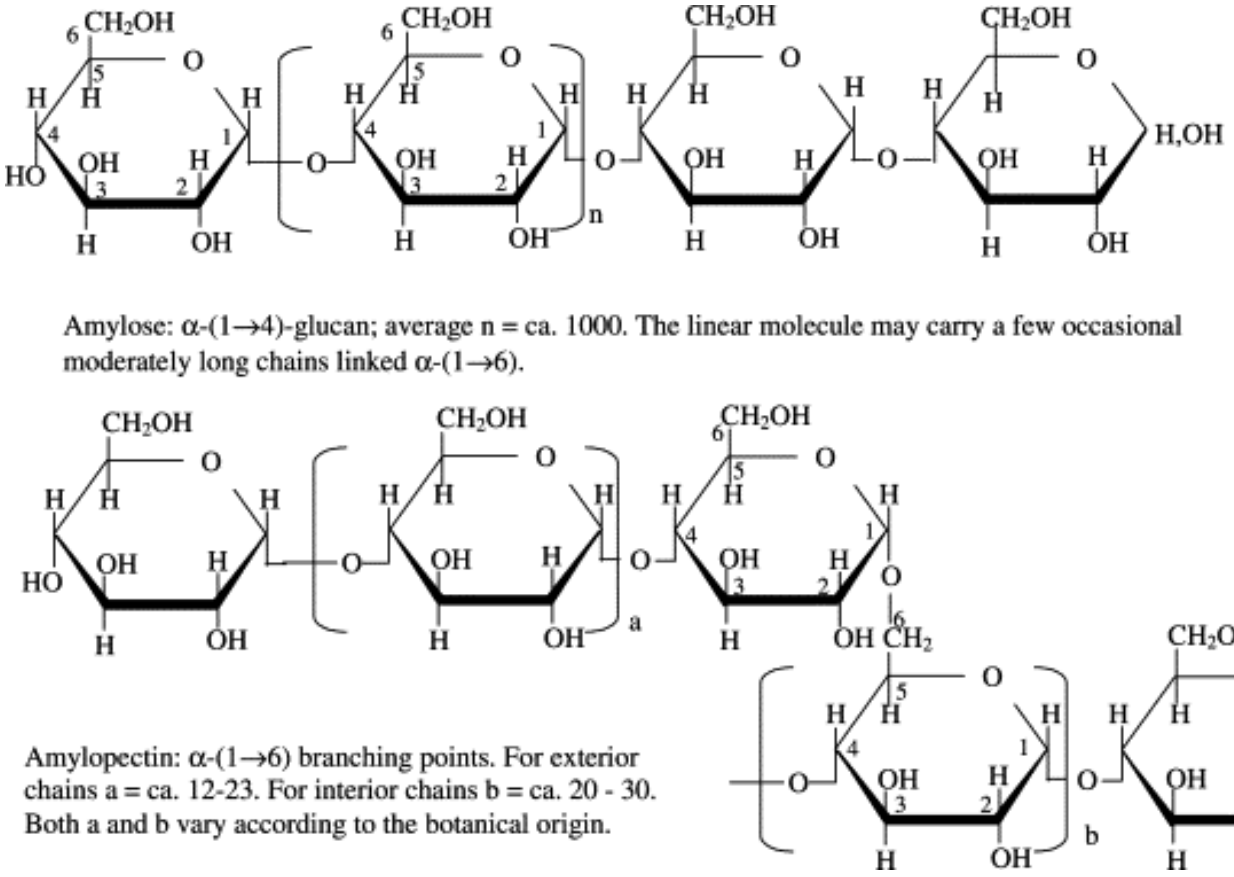

Figure 1. Molecular structure of amylose (upper) and amylopectin (lower). Adapted from Tester et al. (2004).

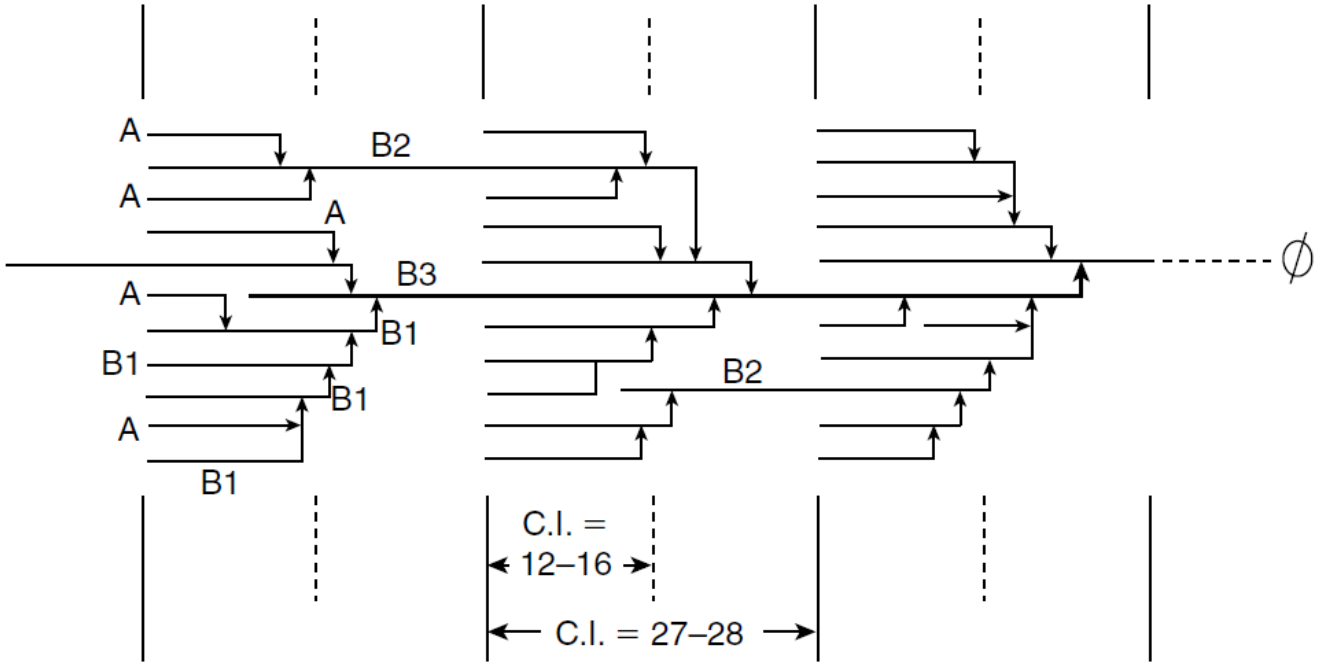

Figure 2. The cluster model of amylopectin adapted from Hizukuri (1986). The straight lines (—) indicate α-(1→4)-linked glucan chains; the arrows express α-(1→6)-linkages or branch points; the Ø symbol depicts the reducing end; c.l. = chain-length.

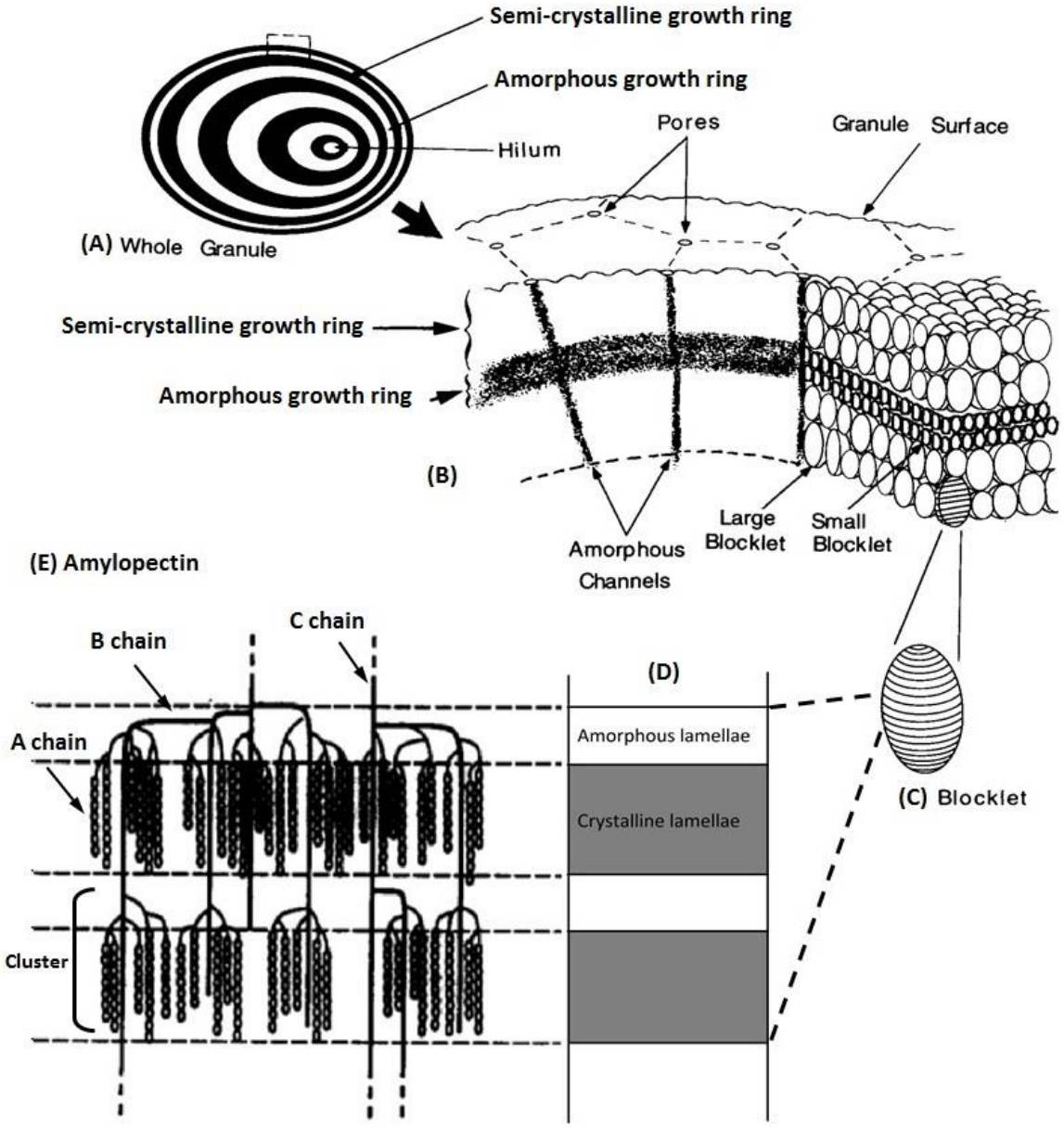

Figure 3. Overview of starch granule structure at different levels of organization: (A) the alternating semi-crystalline (dark) and amorphous (light) growth rings; (B) the proposed arrangement of blocklets comprising semi-crystalline and amorphous growth rings; (C) a blocklet; (D) the alternating crystalline and amorphous lamellae within a blocklet; (E) the molecule of AP with branching regions and double helical chains aligning with alternating amorphous and crystalline lamellae. Adapted from Gallant et al. (1997); Jenkins and Donald (1995).

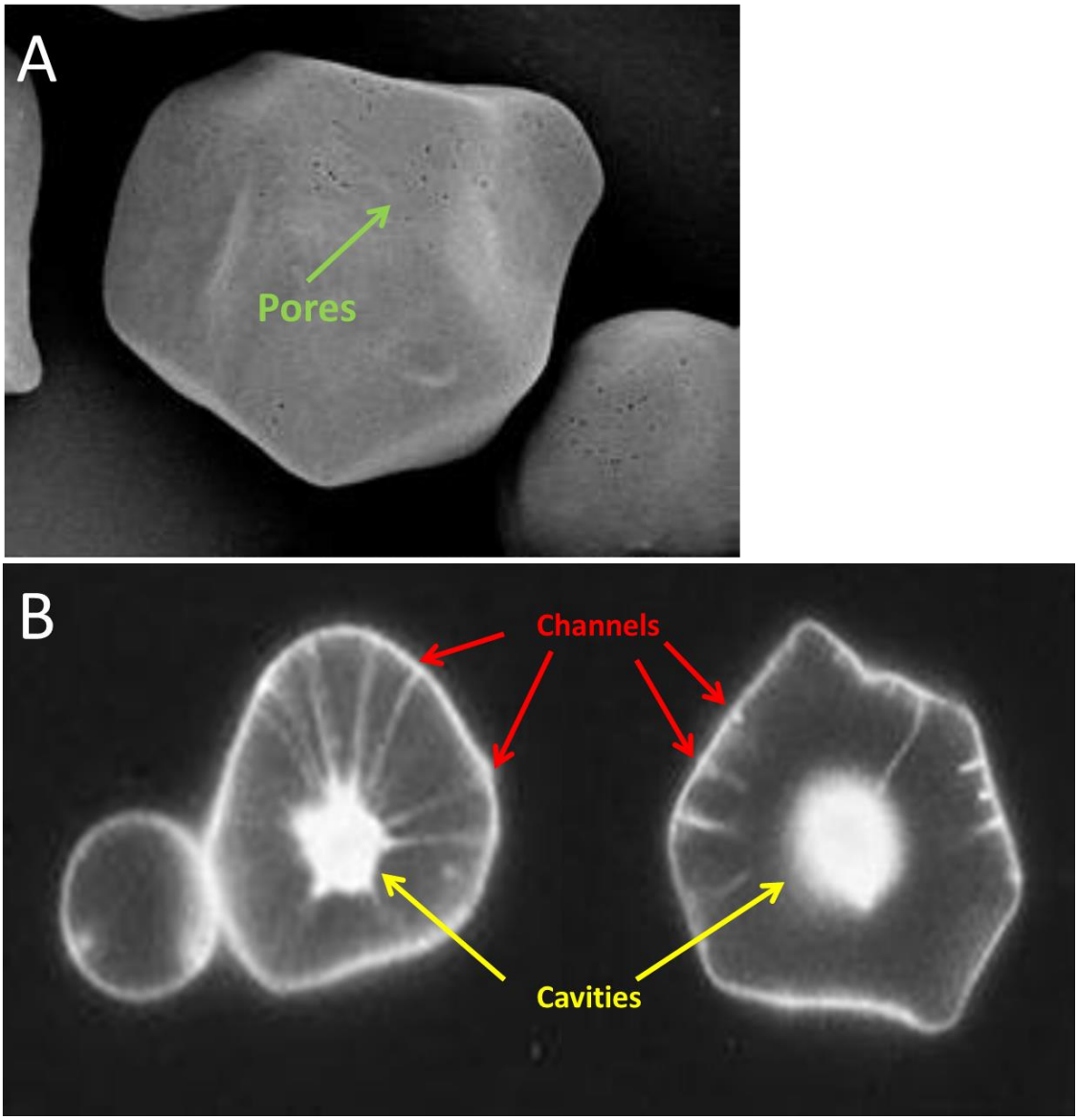

Figure 4. Maize starch granule microstructure: (A) pores at the surfaces of granules viewed by SEM, (B) channels and cavities highlighted by merbromin and viewed by fluorescence microscopy. Adapted from Dhital et al. (2013); Huber and BeMiller (1997); Naguleswaran et al. (2011).

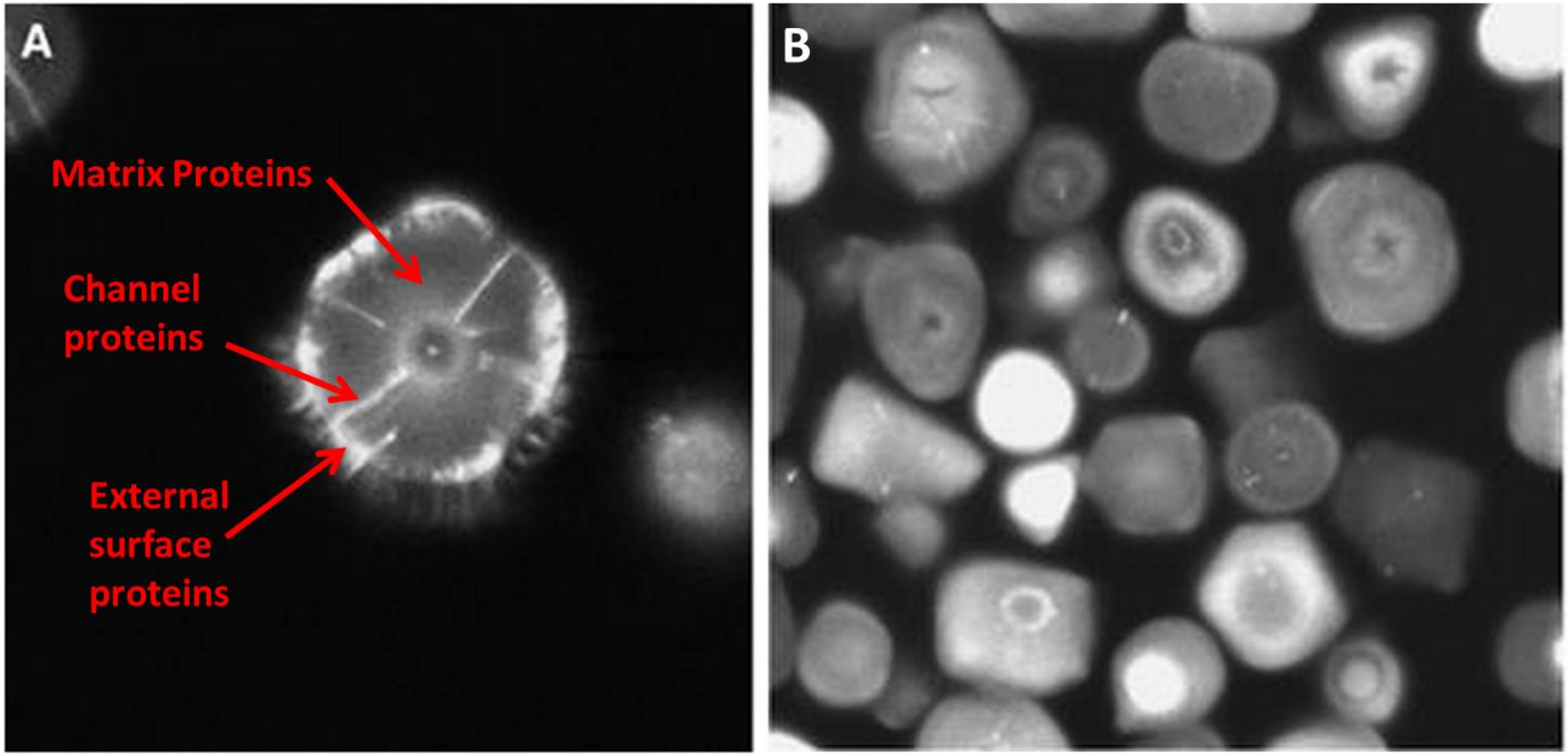

Figure 5. Confocal laser scanning micrographs of CBQCA stained normal maize starch granules: (A) native starch granule with highlighted external surface, channel, and matrix proteins, (B) thermolysin-digested starch granules showing the reduction of CBQCA staining. Adapted from Han et al. (2005).

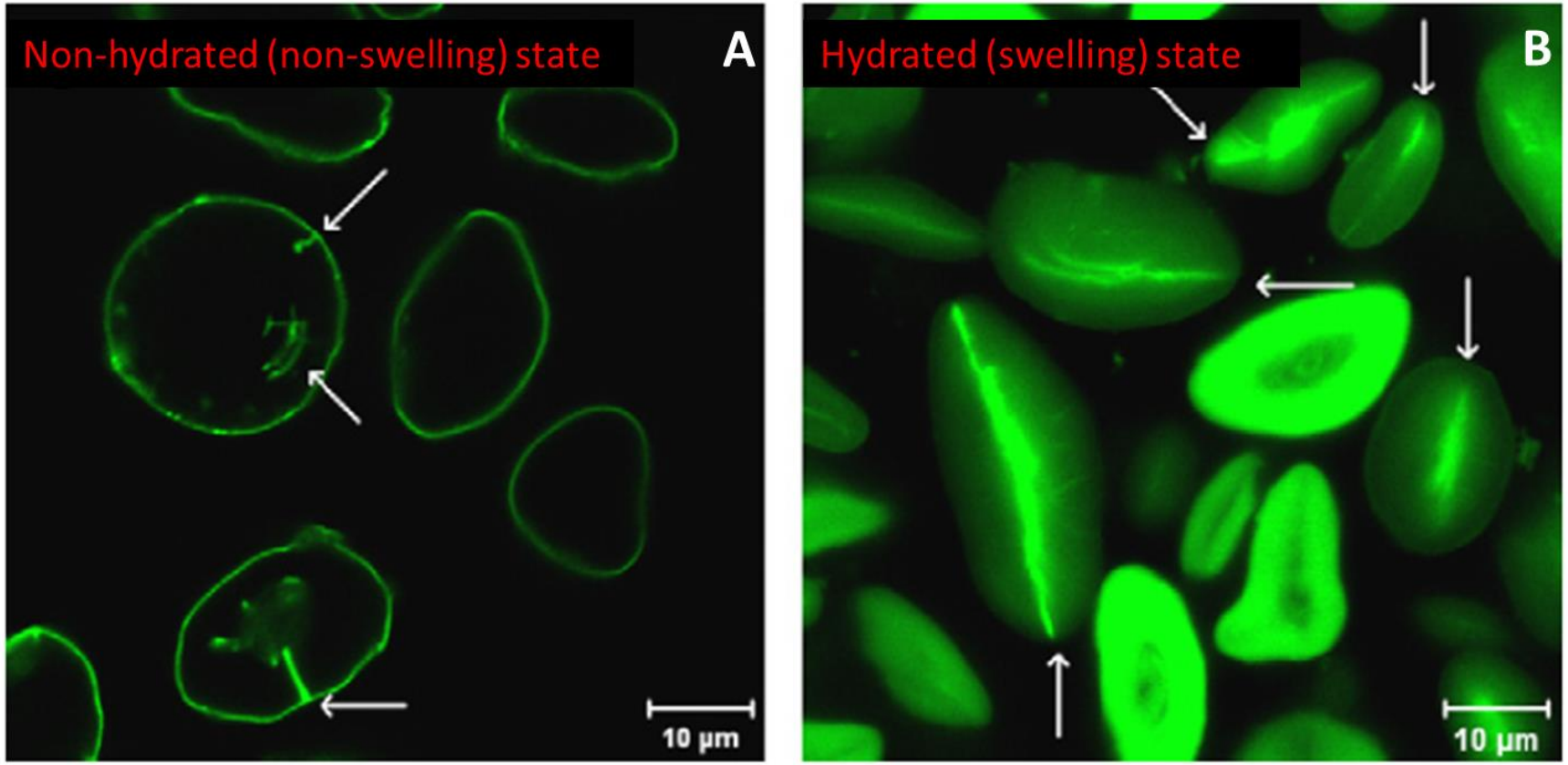

Figure 6. Confocal laser scanning micrographs of normal soft wheat starch granules derivatized with DTAF under (A) non-hydrated or (B) hydrated conditions. Arrows indicate channels and cavities highlighted by DTAF. Adapted from Kim and Huber (2008).

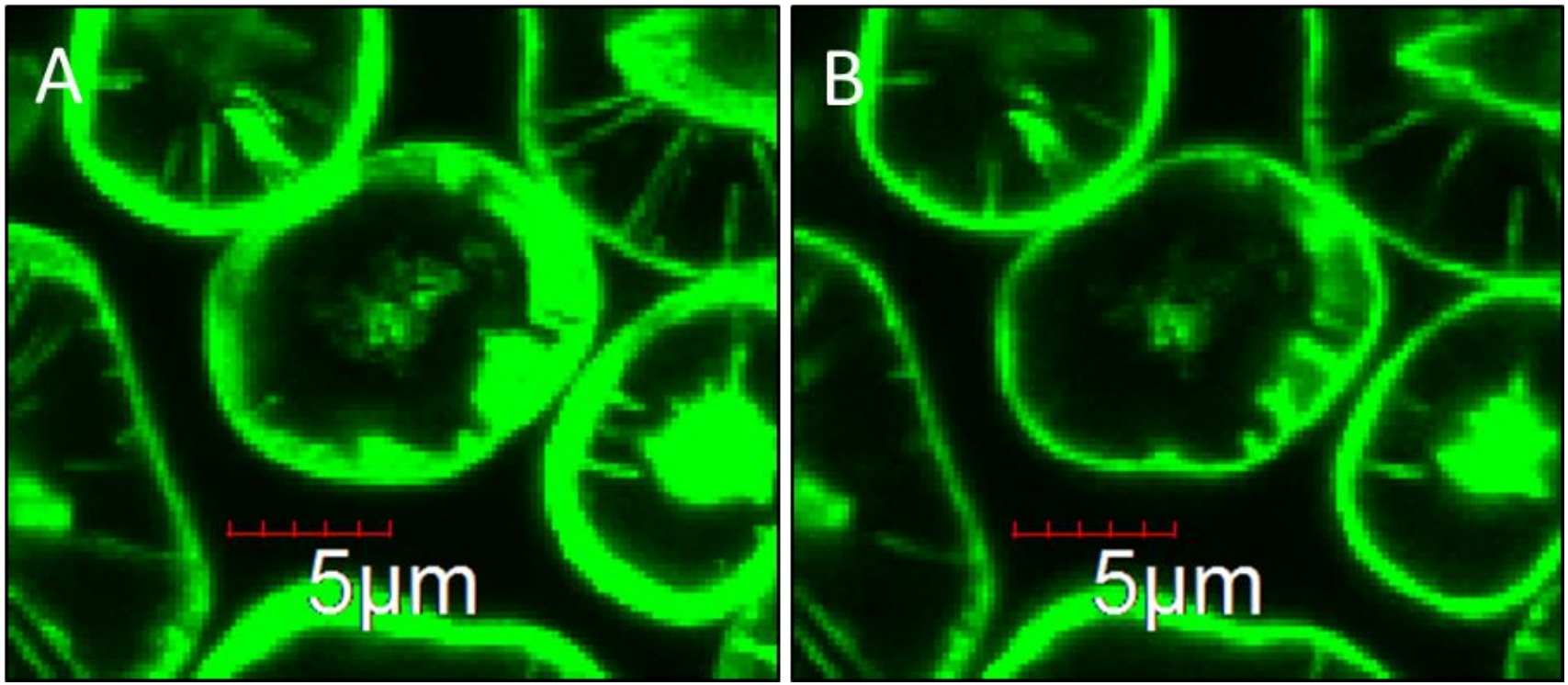

Figure 7. Confocal laser scanning micrographs of merbromin-stained maize starch granules representing (A) a digitally-stacked image of five selected optical cross-sections, (B) a single optical cross-section.

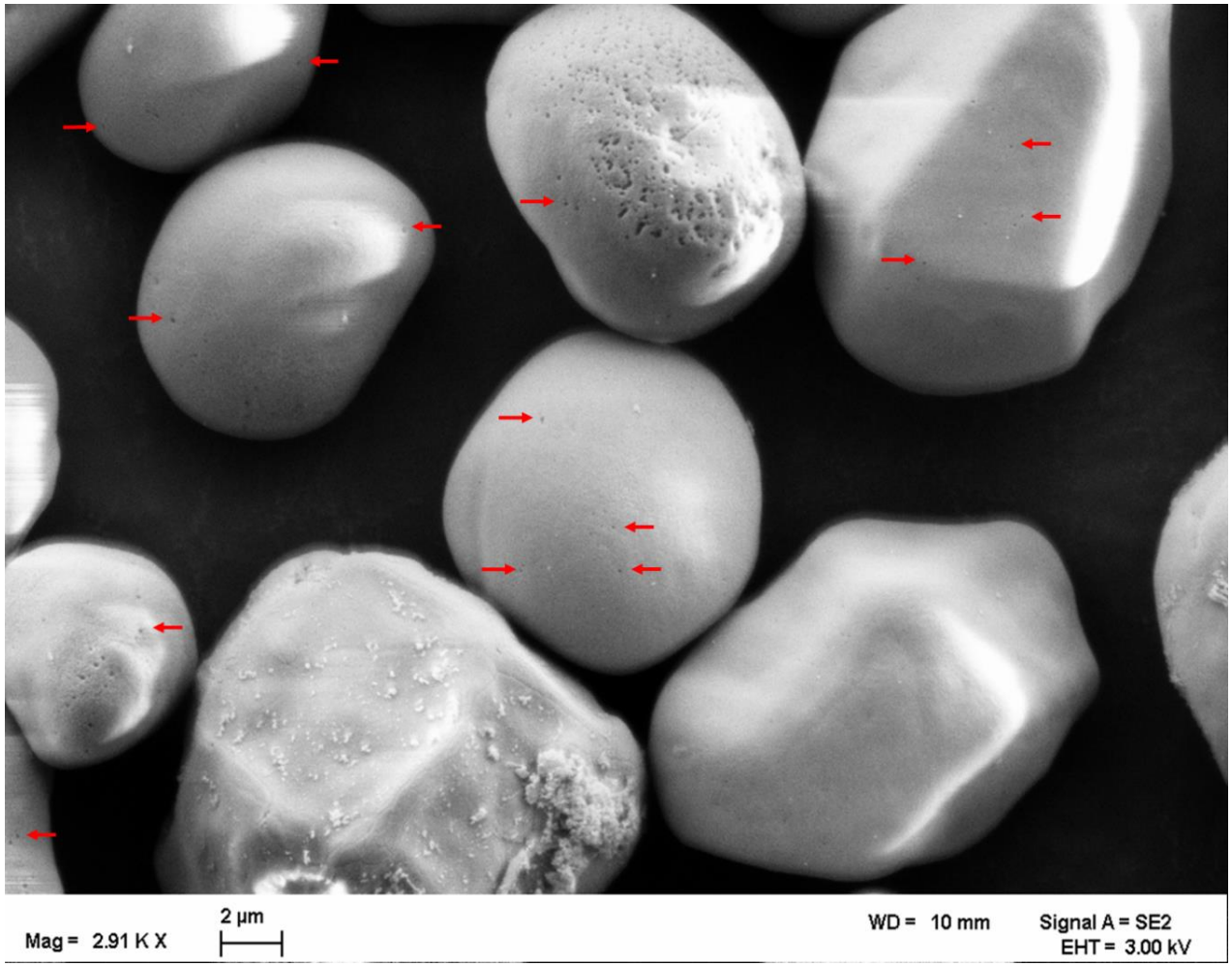

Figure 8. Scanning electron micrograph of native maize (A188 inbred line) starch granules (magnification 2.91 K X, scale bar = 2 µm). Arrows indicate a pore or a cluster of pores on maize starch granules.

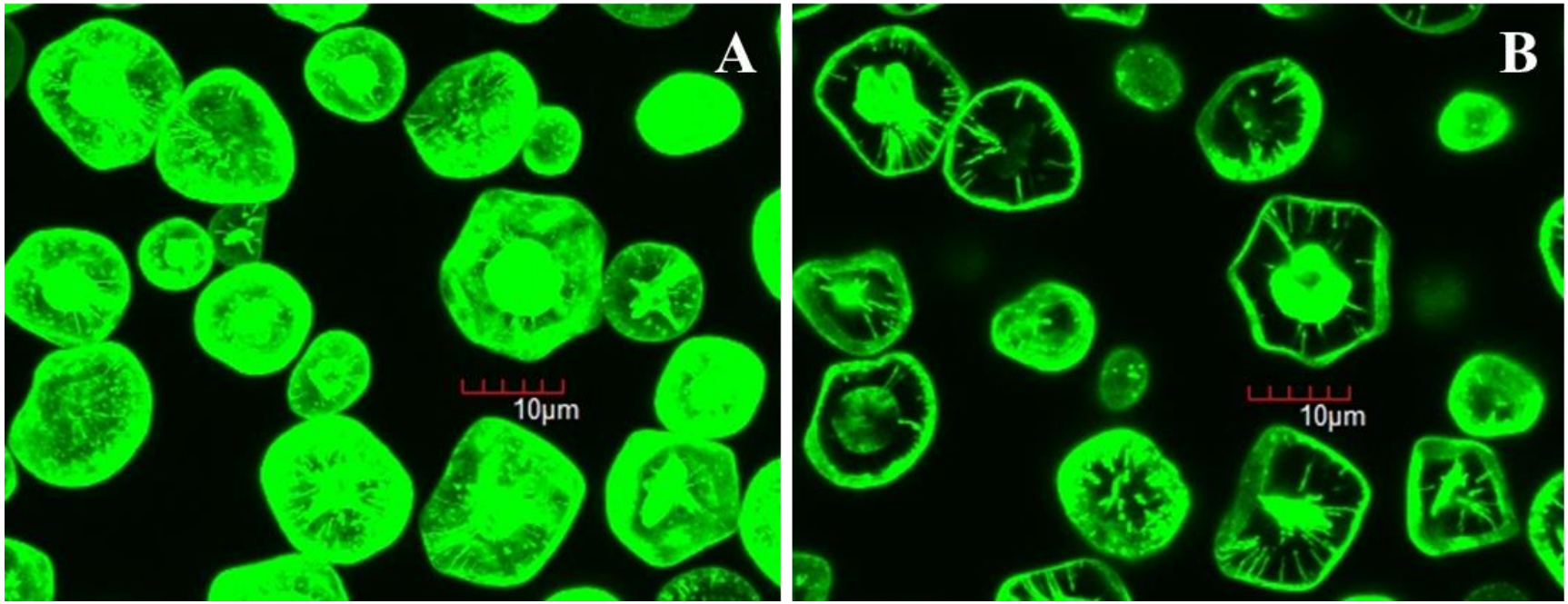

Figure 9. Confocal laser scanning micrographs of merbromin-stained maize starch granules representing (A) the entire set of digitally-stacked serial optical cross-sections, and (B) five select digitally-stacked optical cross-sections representing granule internal regions.

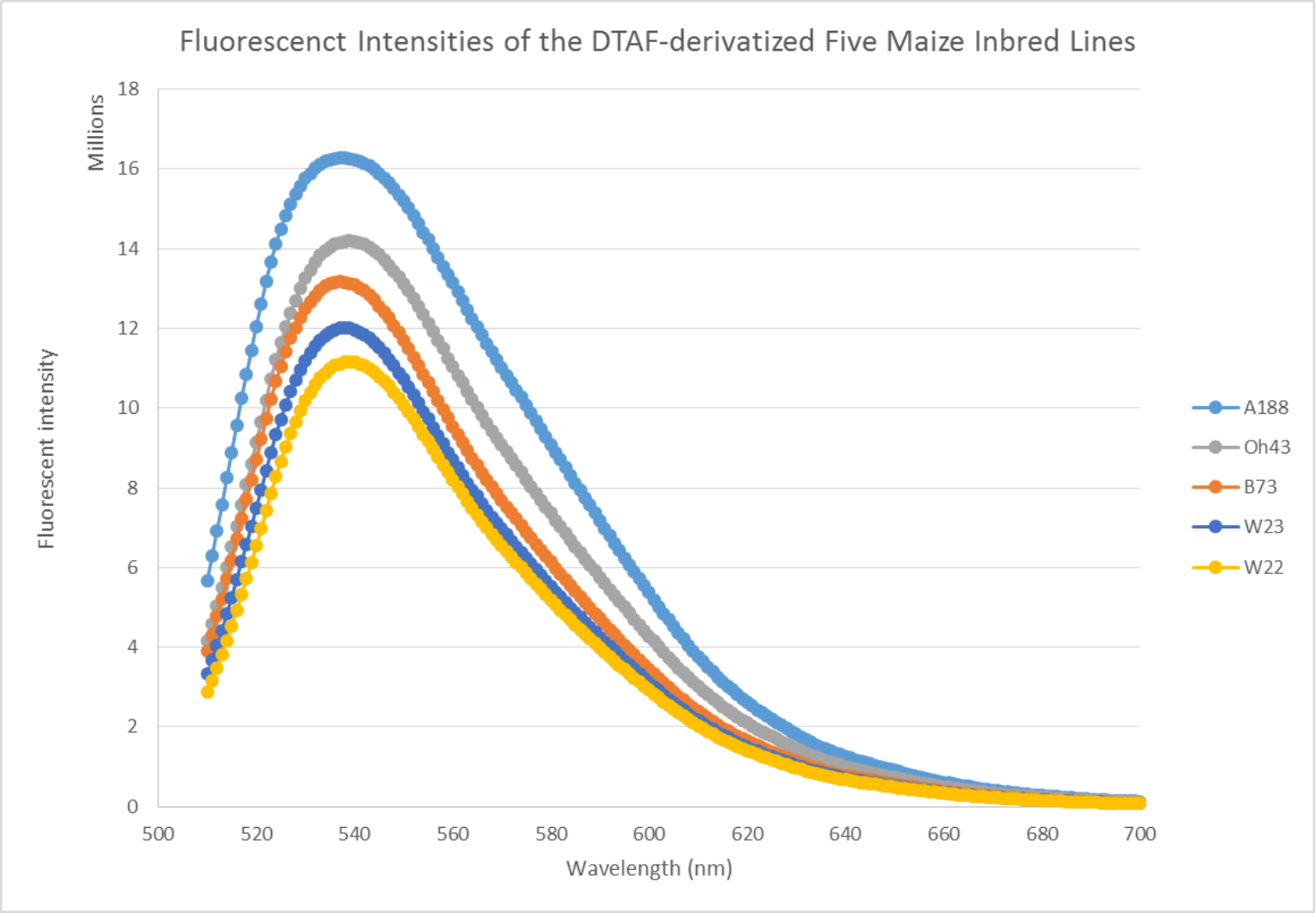

Figure 10. Fluorescent intensities of DTAF-derivatized starch granules of the five maize inbred lines. Fluorescence was achieved at an excitation wavelength of 495 nm and measured at an emission wavelength over the range of 510 – 700 nm.

Table 1. Comparison of RADC rankings determined by channel protein methods. Adapted from Widya et al. (2010).

	Total Channel Protein		**42kDa Channel Marker Protein**		**Actin**	
Maize Starch Source	**Relative[1] Amount of Total Protein**	**RADC Ranking**	**Relative[1] Amount of 42kDa Protein**	**RADC Ranking**	**Relative[1] Amount of Total Protein**	**RADC Ranking**
Oh43	1.9	1	1.5	1	1.9	1
W23	1.75	2	1.2	2	1.75	2
LI[2]	0.4	6	0.6	4	0.4	6
A188	0.7	5	0.5	5	0.7	5
Mo17	1.15	3	0.45	6	1.15	3
W22	1.0	4	1.0	3	1.0	4
B73	0.3	7	0.4	7	0.3	7

[1]All relative amounts of protein are normalized against W22 (assigned reference value of 1.0) and reduced to one decimal point, unless two were needed.

[2]LI = laboratory-isolated normal maize starch. Hybrid unknown.

Table 2. Mean values[1] for starch granule morphological characteristics and RADC estimated by gas adsorption (total specific surface area), manual counting of channels, and DTAF surface reactivity (fluorescence intensity) for starch granules of the five maize inbred lines.

Maize Inbred Line	Granule Diameter (μm)[2]	External Granule Specific Surface Area (m^2/g)[3]	Total Granule Specific Surface Area (m^2/g)[4]	Number of Channels per Granule[5]	Fluorescent intensity[6]
A188	15.55 ± 0.37^{b}	0.2957 ± 0.0061^{b}	6.6770 ± 0.3984^{b}	14.8019 ± 2.8332^{b}	$16.28 \times 10^{6} \pm 0.63 \times 10^{6\ a}$
B73	16.80 ± 0.33^{a}	0.2762 ± 0.0054^{c}	6.4090 ± 0.5166^{b}	11.2308 ± 1.3898^{c}	$13.17 \times 10^{6} \pm 0.36 \times 10^{6\ bc}$
Oh43	14.38 ± 0.10^{c}	0.3150 ± 0.0043^{a}	8.3231 ± 1.2734^{a}	18.5381 ± 1.9544^{a}	$13.48 \times 10^{6} \pm 0.53 \times 10^{6\ b}$
W22	16.46 ± 0.18^{a}	0.2783 ± 0.0034^{c}	6.4159 ± 0.7582^{b}	14.0737 ± 1.4580^{b}	$11.16 \times 10^{6} \pm 0.20 \times 10^{6\ d}$
W23	14.44 ± 0.13^{c}	0.3125 ± 0.0029^{a}	6.0286 ± 0.2065^{b}	11.4888 ± 0.9101^{c}	$12.04 \times 10^{6} \pm 0.47 \times 10^{6\ cd}$

[1]Values within a column sharing a common letter are not significantly different ($p < 0.05$).
[2]Volume% mean granule size determined by particle size analysis.
[3]Estimated mean granule external surface area; calculated from particle size data assuming a spherical granular shape and a hydrated starch density of 1.40 g/ml.
[4]Mean granule specific surface area determined by nitrogen gas adsorption.
[5]Estimated by the manual counting of channels within starch granules.
[6]Based on surface reactivity of starch granules with the fluorescent probe, DTAF.

Table 3. Numbers of starch granules excluded from manual channel counting exercises.

Rationale for Exclusion	**Maize Inbred Line**				
	A188	**B73**	**Oh43**	**W22**	**W23**
Highlighted Cavity/ No Channels[1]	13	37	6	18	23
Damaged/Abnormal Granules[2]	9	16	7	7	10
Indeterminable Features[3]	5	3	4	2	1
Total Excluded Granules	27	56	17	27	34

[1]A highlighted cavity was observed, but without the direct visualization of channels within the constructed image stack.
[2]Granule was damaged or morphological characteristics were abnormal.
[3]Internal granular feature details could not be clearly visualized or a lack of optical cross-sections representing the interior regions of the granule

Table 4. Correlation coefficients (r)[1] among starch granule morphological characteristics and RADC estimated by gas adsorption (total specific surface area), manual counting of channels, and DTAF surface reactivity (fluorescence intensity) for starch granules of the five maize inbred lines.

	Total Specific Surface Area	**Fluorescence Intensity**	**Granule Diameter**	**External Granule Specific Surface Area**	**External Granule Surface Area**
Manual Counting of Channels	0.92*	0.29	-0.45	0.45	-0.69
Total Specific Surface Area		0.25	-0.44	0.47	-0.64
Fluorescence Intensity			-0.10	0.15	-0.47
Granule Diameter				-0.99*	0.89*
External Granule Specific Surface Area					-0.91

[1]*Significant at $p < 0.05$; n = 5.

Table 5. Specific surface area values for starches of maize inbred lines W22 and W23 measured by gas adsorption at different degassing temperatures.

Maize Inbred Line	**Degassing Temperature**		
	40 °C	**90 °C**	**120 °C**
W22	0.729±0.0076	0.836±0.0090	6.416±0.7582
W23	0.867±0.0074	0.974±0.0089	6.029±0.2065

Table 6. Comparison of the RADC rankings for starches of the five maize inbred lines established via manual channel counting, gas adsorption (total specific surface area), and DTAF surface reaction (fluorescence intensity) methods in relation to the channel protein methods established by Widya et al. (2010).

	RADC Ranking					
Maize Inbred Line	**Manual Counting of Channels**	**Total Granule Specific Surface Area**	**Fluorescence Intensity**	**Total Channel Protein**	**42kDa Channel Marker Protein**	**Actin**
Oh43	1	1	2	1	1	1
A188	2	2	1	4	4	3
W22	3	3	5	3	3	4
W23	4	5	4	2	2	2
B73	5	4	3	5	5	5

Table 7. Correlation coefficients (r)[1] among RADC established via gas adsorption (total specific surface area), manual counting of channels, and DTAF surface reactivity (fluorescence intensity) for starch granules of the five maize inbred lines, and RADC determined via channel protein methods established by Widya et al. (2010).

	Total Specific Surface Area	**Fluorescence Intensity**	**Total Channel Protein**	**42kDa Channel Marker Protein**	**Actin**
Manual Counting of Channels	0.92*	0.29	0.48	0.55	0.39
Total Specific Surface Area		0.25	0.46	0.53	0.44
Fluorescence Intensity			-0.29	-0.44	0.06
Total Channel Protein				0.96*	0.89*
42kDa Channel Marker Protein					0.15

[1]*Significant at $p < 0.05$; n = 5.

7.0. LITERATURE CITED

Ahmed, M., Stal, L. J. and Hasnain, S. 2011. DTAF: an efficient probe to study cyanobacterial-plant interaction using confocal laser scanning microscopy (CLSM). Journal of Industrial Microbiology & Biotechnology 38:249-255.

Aranda, A. I., Achelle, S., Hammerer, F., Mahuteau-Betzer, F. and Teulade-Fichou, M.-P. 2012. Vinyl-diazine triphenylamines and their N-methylated derivatives: Synthesis, photophysical properties and application for staining DNA. Dyes and Pigments 95:400-407.

Baldwin, P. M. 2001. Starch granule-associated proteins and polypeptides: A review. Starch-Starke 53:475-503.

Baldwin, P. M., Adler, J., Davies, M. C. and Melia, C. D. 1998. High resolution imaging of starch granule surfaces by atomic force microscopy. Journal of Cereal Science 27:255-265.

Baldwin, P. M., Davies, M. C. and Melia, C. D. 1997. Starch granule surface imaging using low-voltage scanning electron microscopy and atomic force microscopy. International Journal of Biological Macromolecules 21:103-107.

BeMiller, J. N. and Huber, K. C. 2012. Starch. Pages 113-141 in: Ullmann's Encyclopedia of Industrial Chemistry. Wiley-VCH Verlag GmbH & Co. KGaA: Weinheim.

Benmoussa, M., Hamaker, B. R., Huang, C. P., Sherman, D. M., Weil, C. F. and BeMiller, J. N. 2010. Elucidation of maize endosperm starch granule channel proteins and evidence for plastoskeletal structures in maize endosperm amyloplasts. Journal of Cereal Science 52.

Blazek, J. and Gilbert, E. P. 2011. Application of small-angle X-ray and neutron scattering techniques to the characterisation of starch structure: A review. Carbohydrate Polymers 85:281-293.

Buleon, A., Colonna, P., Planchot, V. and Ball, S. 1998. Starch granules: structure and biosynthesis. International Journal of Biological Macromolecules 23:85-112.

Cano, A., Jimenez, A., Chafer, M., Gonzalez, C. and Chiralt, A. 2014. Effect of amylose:amylopectin ratio and rice bran addition on starch films properties. Carbohydrate Polymers 111:543-555.

Dhital, S., Shelat, K. J., Shrestha, A. K. and Gidley, M. J. 2013. Heterogeneity in maize starch granule internal architecture deduced from diffusion of fluorescent dextran probes. Carbohydrate Polymers 93:365-373.

Dhital, S., Shrestha, A. K. and Gidley, M. J. 2010. Relationship between granule size and in vitro digestibility of maize and potato starches. Carbohydrate Polymers 82:480-488.

Fannon, J. E., Gray, J. A., Gunawan, N., Huber, K. C. and BeMiller, J. N. 2004. Heterogeneity of starch granules and the effect of granule channelization on starch modification. Cellulose 11:247-254.

Fannon, J. E., Hauber, R. J. and Bemiller, J. N. 1992. Surface pores of starch granules. Cereal Chemistry 69:284-288.

Fannon, J. E., Shull, J. M. and Bemiller, J. N. 1993. Interior channels of starch granules. Cereal Chemistry 70:611-613.

Fortuna, T., Januszewska, R., Juszczak, L., Kielski, A. and Palasinski, M. 2000. The influence of starch pore characteristics on pasting behaviour. International Journal of Food Science and Technology 35:285-291.

Gallant, D. J., Bouchet, B. and Baldwin, P. M. 1997. Microscopy of starch: evidence of a new level of granule organization. Carbohydrate Polymers 32:177-191.

Geera, B. P., Nelson, J. E., Souza, E. and Huber, K. C. 2006. Granule bound starch synthase I (GBSSI) gene effects related to soft wheat flour/starch characteristics and properties. Cereal Chemistry 83:544-550.

Gray, J. A. and BeMiller, J. N. 2004. Development and utilization of reflectance confocal laser scanning microscopy to locate reaction sites in modified starch granules. Cereal Chemistry 81:278-286.

Han, X. Z., Benmoussa, M., Gray, J. A., BeMiller, J. N. and Hamaker, B. R. 2005. Detection of proteins in starch granule channels. Cereal Chemistry 82.

Han, X. Z. and Hamaker, B. R. 2002. Location of starch granule-associated proteins revealed by confocal laser scanning microscopy. Journal of Cereal Science 35:109-116.

Hellman, N. N. and Melvin, E. H. 1950. Surface area of starch and its role in water sorption. Journal of the American Chemical Society 72:5186-5188.

Hizukuri, S. 1985. Relationship between the Distribution of the Chain Length of Amylopectin and the Crystalline Structure of Starch Granules. Carbohydrate Research 141:295-306.

Hizukuri, S. 1986. Polymodal distribution of the chain lengths of amylopectins, and its significance. Carbohydrate Research 147:342-347.

Hoover, R. 2001. Composition, molecular structure, and physicochemical properties of tuber and root starches: a review. Carbohydrate Polymers 45:253-267.

Huber, K. C. and BeMiller, J. N. 1997. Visualization of channels and cavities of corn and sorghum starch granules. Cereal Chemistry 74:537-541.

Huber, K. C. and BeMiller, J. N. 2000. Channels of maize and sorghum starch granules. Carbohydrate Polymers 41:269-276.

Huber, K. C. and BeMiller, J. N. 2001. Location of sites of reaction within starch granules. Cereal Chemistry 78:173-180.

Huber, K. C. and BeMiller, J. N. 2010. Chapter 8 Modified starch: Chemistry and properties in: Starches: Characterization, Properties, and Applications. A. C. Bertolini, ed. CRC Press: Hoboken.

Jacobs, H. and Delcour, J. A. 1998. Hydrothermal modifications of granular starch, with retention of the granular structure: A review. Journal of agricultural and food chemistry 46:2895-2905.

Jenkins, J. P. J., Cameron, R. E. and Donald, A. M. 1993. A universal feature in the structure of starch granules from different botanical sources. Starch-Starke 45:417-420.

Jenkins, P. J. and Donald, A. M. 1995. The influence of amylose on starch granule structure. International Journal of Biological Macromolecules 17:315-321.

Juszczak, L., Fortuna, T. and Krok, F. 2003a. Non-contact atomic force microscopy of starch granules surface. Part I. Potato and tapioca starches. Starch-Starke 55:1-7.

Juszczak, L., Fortuna, T. and Krok, F. 2003b. Non-contact atomic force microscopy of starch granules surface. Part II. Selected cereal starches. Starch-Starke 55:8-16.

Juszczak, L., Fortuna, T. and Wodnicka, K. 2002. Characteristics of cereal starch granules surface using nitrogen adsorption. Journal of Food Engineering 54:103-110.

Kim, H. S. and Huber, K. C. 2006. Alkaline dissolution of starch facilitated by microwave heating for analysis by size-exclusion chromatography. Journal of agricultural and food chemistry 54:9664-9669.

Kim, H. S. and Huber, K. C. 2008. Channels within soft wheat starch A- and B-type granules. Journal of Cereal Science 48:159-172.

Kim, H. S. and Huber, K. C. 2010. Physicochemical properties and amylopectin fine structures of A- and B-type granules of waxy and normal soft wheat starch. Journal of Cereal Science 51:256-264.

Klobes, P., Meyer, K., Munro, R. G., National Institute of, S. and Technology. 2006. Porosity and specific surface area measurements for solid materials. U.S. Dept. of Commerce,

Technology Administration, National Institute of Standards and Technology: [Gaithersburg, Md.].

Kong, B. W., Kim, J. I., Kim, M. J. and Kim, J. C. 2003. Porcine pancreatic alpha-amylase hydrolysis of native starch granules as a function of granule surface area. Biotechnology Progress 19:1162-1166.

Kossmann, J. and Lloyd, J. 2000. Understanding and influencing starch biochemistry. Critical Reviews in Plant Sciences 19:171-226.

Lee, S.-H. and BeMiller, J. N. 2008. Lysophosphatidylcholine Identified as Channel-Associated Phospholipid of Maize Starch Granules. Cereal Chemistry 85.

Li, E. P., Dhital, S. and Hasjim, J. 2014. Effects of grain milling on starch structures and flour/starch properties. Starch-Starke 66:15-27.

Lindeboom, N., Chang, P. R. and Tyler, R. T. 2004. Analytical, biochemical and physicochemical aspects of starch granule size, with emphasis on small granule starches: A review. Starch-Starke 56:89-99.

Naguleswaran, S., Li, J. H., Vasanthan, T. and Bressler, D. 2011. Distribution of granule channels, protein, and phospholipid in triticale and corn starches as revealed by confocal laser scanning microscopy. Cereal Chemistry 88:87-94.

Naguleswaran, S., Li, J. H., Vasanthan, T., Bressler, D. and Hoover, R. 2012. Amylolysis of large and small granules of native triticale, wheat and corn starches using a mixture of alpha-amylase and glucoamylase. Carbohydrate Polymers 88:864-874.

Oates, C. G. 1997. Towards an understanding of starch granule structure and hydrolysis. Trends in Food Science & Technology 8:375-382.

Oostergetel, G. T. and Vanbruggen, E. F. J. 1993. The crystalline domains in potato starch granules are arranged in a helical fashion. Carbohydrate Polymers 21:7-12.

Ozturk, S. and Koksel, H. 2014. Production and characterisation of resistant starch and its utilisation as food ingredient: a review. Quality Assurance and Safety of Crops & Foods 6:335-346.

Perez, S. and Bertoft, E. 2010. The molecular structures of starch components and their contribution to the architecture of starch granules: A comprehensive review. Starch-Starke 62:389-420.

Robin, J. P., Mercier, C., Charbonn.R and Guilbot, A. 1974. Lintnerized starches. Gel filtration and enzymatic studies of insoluble residues from prolonged acid treatment of potato starch. Cereal Chemistry 51:389-406.

Salman, H., Blazek, J., Lopez-Rubio, A., Gilbert, E. P., Hanley, T. and Copeland, L. 2009. Structure-function relationships in A and B granules from wheat starches of similar amylose content. Carbohydrate Polymers 75:420-427.

Schumann, R. and Rentsch, D. 1998. Staining particulate organic matter with DTAF - a fluorescence dye for carbohydrates and protein: a new approach and application of a 2D image analysis system. Marine Ecology Progress Series 163:77-88.

Schwartz, D. and Whistler, R. L. 2009. Chapter 1 - History and Future of Starch. Pages 1-10 in: Starch (Third Edition). J. BeMiller and R. Whistler, eds. Academic Press: San Diego.

Siegler, R., Sternson, L. A. and Stobaugh, J. F. 1989. Suitability of DTAF as a fluorescent labelling reagent for direct analysis of primary and secondary amines — spectral and chemical reactivity considerations. Journal of Pharmaceutical and Biomedical Analysis 7:45-55.

Singh, J., Kaur, L. and McCarthy, O. J. 2007. Factors influencing the physico-chemical, morphological, thermal and rheological properties of some chemically modified starches for food applications - A review. Food Hydrocolloids 21:1-22.

Singh, N., Singh, J., Kaur, L., Sodhi, N. S. and Gill, B. S. 2003. Morphological, thermal and rheological properties of starches from different botanical sources. Food Chemistry 81:219-231.

Soulaka, A. B. and Morrison, W. R. 1985. The amylose and lipid contents, dimensions, and gelatinisation characteristics and some wheat starches and their A- and B-granule fractions. Journal of the Science of Food and Agriculture 36:709-718.

Sui, Z. Q. and BeMiller, J. N. 2013. Relationship of the channels of normal maize starch to the properties of its modified products. Carbohydrate Polymers 92:894-904.

Sui, Z. Q., Shah, A. and Miller, J. N. B. 2011. Crosslinked and stabilized in-kernel heat-moisture-treated and temperature-cycled normal maize starch and effects of reaction conditions on starch properties. Carbohydrate Polymers 86:1461-1467.

Sujka, M. and Jamroz, J. 2007. Starch granule porosity and its changes by means of amylolysis. International Agrophysics 21:107-113.

Sujka, M. and Jamroz, J. 2009. alpha-Amylolysis of native potato and corn starches - SEM, AFM, nitrogen and iodine sorption investigations. Lwt-Food Science and Technology 42:1219-1224.

Tester, R. F., Karkalas, J. and Qi, X. 2004. Starch - composition, fine structure and architecture. Journal of Cereal Science 39:151-165.

Widya, Y., Gunawan, N. and BeMiller, J. N. 2010. Methods for determining relative average number of channels per maize starch granule and digestion of raw granules of mutant maize cultivars by amyloglucosidase. Cereal Chemistry 87:194-203.

Wongsagonsup, R., Varavinit, S. and BeMiller, J. N. 2008. Increasing Slowly Digestible Starch Content of Normal and Waxy Maize Starches and Properties of Starch Products. Cereal Chemistry 85:738-745.

Xie, F. W., Pollet, E., Halley, P. J. and Averous, L. 2013. Starch-based nano-biocomposites. Progress in Polymer Science 38:1590-1628.

Yuryev, V. P., Krivandin, A. V., Kiseleva, V. I., Wasserman, L. A., Genkina, N. K., Fornal, J., Blaszczak, W. and Schiraldi, A. 2004. Structural parameters of amylopectin clusters and semi-crystalline growth rings in wheat starches with different amylose content. Carbohydrate Research 339:2683-2691.